Experiment 231: Revised Proposal
Correspondent: R. Yamada
NAL
Batavia, Illinois

Telephone FTS/Commercial:
312-840-3252

p-p and p-d Elastic and Inelastic Scattering in the New C0 Internal Target Laboratory

Y. Akimov, A. Kuznetsov, B. Morozov, S. Mukhin,
V. Nikitin, Y. Pilipenko, V. Tsarev, and L. Zolin
Joint Institute for Nuclear Research (Dubna)

and

E. Malamud, R. Yamada, and P. Zimmerman
National Accelerator Laboratory

and

F. Loeffler, E. Shibata, K. Stanfield, and Y. Tang
Purdue University

March 7, 1974

ABSTRACT

We propose an experiment to measure p-p and p-d elastic and inelastic scattering in the new C0 Internal Target Area. These measurements will cover the t-region from 0.2 up to 10 $(GeV/c)^2$ for p-p elastic scattering and up to 5 $(GeV/c)^2$ for p-d elastic scattering. Incident beam energies from 8 to 500 GeV will be continuously covered. A magnetic spectrometer will be used to measure the angles and momenta of the recoil particles. In the higher t-region a forward hodoscope (or a forward magnetic spectrometer in later stages of the experiment) will be used to identify elastic from inelastic events. For absolute normalization we will install solid state detectors, which will cover both the Coulomb and nuclear scattering regions.

INDEX

I. INTRODUCTION

In July 1973 we submitted experimental proposal 231 "p-p and p-d Elastic and Inelastic Scattering in the High t-region in the New Internal Target Laboratory". In this proposal we planned to do p-p and p-d elastic and inelastic scattering using a hydrogen and deuterium jet target at the B0 straight section, which we assumed would be expanded into a bigger internal target area at that time.

During the 1973 Summer Study, the subject of expanding an internal target area was discussed. As a result of the discussion, D. Jovanovic, E. Malamud, V. Nikitin, and A. Kuznetsov[1] have proposed construction of a modest experimental hall at C0 which might house the recoil spectrometer proposed in Exp. 231. In light of these developments, we reexamined our proposal and concluded that the experiment was feasible in the new C0 laboratory and that certain improvements were possible with only minor modifications. At that time we wrote a letter to urge the start of construction at C0 and the approval of our experimental proposal.

During this time Exp. 36 was finished and Exp. 186 was started in the present C0 area using the jet target. In Exp. 36 members of our collaboration measured the slope parameter, b, and the ratio of the real to the imaginary part of the scattering amplitude for p-p elastic scattering.[2,3] The diffraction excitation of nucleon resonances in p-p collision at incident proton energies from 175 to 400 GeV were also measured.[4] In Exp. 186 p-d elastic and inelastic scattering up to $|t| = 0.2$ $(GeV/c)^2$ is being measured, and these data are being processed now.

It is now clear that the jet target has been very fruitful for the investigation of not only elastic scattering but also inelastic scattering. The jet target has also been used by other experimental groups to measure the p+p → p+X inclusive reaction[5] and the p+p → γ+X reaction.[6] In the internal target area we have the added advantage that all incident energies are readily available up to the maximum machine energy. The s-dependence of the reactions can be determined easily.

We believe that a large variety of physics can be studied in the expanded internal target laboratory. Using a magnetic spectrometer as the basic apparatus, a series of experiments which require only minor modifications or additions to the apparatus will be done.

As a first experiment we wish to measure p-p and p-d elastic and inelastic scattering in two phases (I and II). Members of our collaboration have already studied the low t-region (up to $|t| \approx 0.2$ $(GeV/c)^2$) with solid state detectors; this experiment would extend the t-region to $|t| = 10$ $(GeV/c)^2$ for p-p scattering and to $|t| = 5$ $(GeV/c)^2$ for p-d scattering.

In the first phase, we should like to measure the t-range from 0.2 to 5 $(GeV/c)^2$ for p-p scattering and up to 3 $(GeV/c)^2$ for p-d scattering. During Phase I we will use the recoil magnetic spectrometer and install a scintillation counter hodoscope in the forward direction. With this hodoscope we will study counting rates and investigate the power of coplanarity and opening angle constraints. This study will pave the way for extending the measurements to t values larger than 5 $(GeV/c)^2$ and will also improve the lower t measurements.

In Phase II we will use a forward magnetic spectrometer to extend the measurements to $|t| = 10$ $(GeV/c)^2$ for the p-p reaction and to 5 $(GeV/c)^2$ for the p-d reaction.

We will install an absolute monitor system using solid state detectors to measure the elastic scattering in the nuclear scattering region and also in the Coulomb scattering region. Thus, we will have the ability to absolutely normalize the data.

Most of the equipment which we propose can be used for many future experiments, including these same experiments extended to 1000 GeV when the proposed energy doubler comes into operation. The new C0 laboratory will be used by many other experiments, and will be the first experimental area for the beam from the energy doubler.

To summarize, the physics which we propose to study is as follows:

1. Elastic p-p scattering in the t-region from $|t| = 0.2$ to 5 $(GeV/c)^2$ for energies from 8 to 500 GeV and elastic pd scattering to $|t| = 3$ $(GeV/c)^2$ (Phase I).
2. Isobar production in p-p and p-d scattering in the same region as above (Phase I).
3. The inclusive reactions $pp \rightarrow pX$ and $pd \rightarrow dX$ with the recoiling proton and deuteron momentum up to 6 GeV/c (Phase I).
4. Elastic p-p scattering in the t-region from 5 to 10 $(GeV/c)^2$ for energies from 50 to 500 GeV, and elastic p-d scattering in the t-region from 3 to 5 $(GeV/c)^2$ (Phase II).

II. PHYSICS

Elastic scattering may be divided into regions according to the t-range covered as shown in Table 1 for p-p elastic scattering and Table 2 for p-d elastic scattering. The data are divided according to their phenomenological behavior. Regions 1 and 2, for p-p and p-d, are measured in Experiment 36 and 186. We will extend these measurements in the new internal target laboratory to higher t and s-regions.

A. p-p Elastic Scattering

Elastic p-p scattering at very high energy and up to $|t| = 5$ $(GeV/c)^2$ has been measured at the ISR and reported[7] as shown in Fig. 1. Extensive data exists below 30 GeV, but there is not enough data between 30 GeV and ISR energies. We can measure elastic scattering in the NAL energy range and thereby provide this fundamental data in the gap between 30 GeV and ISR energies.

The most prominent feature of the ISR data is the dip around 1.3 $(GeV/c)^2$ as shown in Fig. 1. This had not been observed at lower energies, although a kink in the cross sections exists there. This dip was predicted by many models.[8] According to theory, this dip is partially filled at low energy where the real part of the scattering amplitude and non-diffractive contributions are large. Experiment 36 finds the ratio of the real to the imaginary part of the scattering amplitude to cross zero at 280 ± 60 GeV, as shown in Fig. 2. Therefore, we can expect to be able to observe this dip and investigate the s-dependence of its depth and position at NAL energies. Its relation to the real part of the scattering amplitude will be studied.

An interesting prediction for the shape of the dip has been published by Phillips and Barger,[9] who did a model independent analysis of the data in terms of two exponential amplitudes with a relative phase. The steeper exponential has normal Regge shrinkage and phase, while the other does not shrink. As indicated in Fig. 3, their picture predicts the deepest dip near 175 GeV.

The height of the second maximum varies according to different models. For example, the Chou-Yang model predicts a rise in $d\sigma/dt$ at $|t| = 1.8$ $(GeV/c)^2$ while Regge models predict no rise for the secondary peak. Measurements in this region will distinguish between these models.

Some theories predict a second dip around $|t| = 5 \sim 8$ $(GeV/c)^2$. If this dip exists, our counting rate is high enough to find it. In this regard the internal target has an advantage over the ISR. As is described in a memo by E. Malamud,[10] the interaction rate per second for $\sigma = 40$ mb is 10^4 for the ISR with a 10 ampere current, while that of a jet target is 7×10^8 with a proton density of 5×10^{-7} g/cm^3 and a beam intensity of 10^{13} ppp. Thus, our rate is about 10^5 higher than that of the ISR. We will have improved statistics and will be able to measure into the higher t-region where the cross section is smaller. The data of Fig. 1 ends around $|t| \approx 5$ $(GeV/c)^2$. We will be able to extend these results to $|t| \approx 10$ $(GeV/c)^2$.

B. p-d Elastic Scattering

The differential cross section for p-d elastic scattering was measured up to $|t| = 2$ $(GeV/c)^2$ at CERN using the PS up to 24 GeV/c.[11] This result is shown in Fig. 4. The region near

$|t| = 0.3$ $(GeV/c)^2$, where a dip is expected, has been investigated at lower energies extensively in other laboratories. Only a kink has been found which was attributed to the d-state admixture.[12] Beyond $|t| = 2$ $(GeV/c)^2$ no data exists even at low energy. Only the NAL machine has the capability to investigate this region.

At $|t| \gtrsim 0.35$ $(GeV/c)^2$ the double scattering term in the p-d scattering amplitude dominates. At small s this term is determined mainly by elastic rescattering (elastic Glauber corrections). However, at higher energies inelastic contributions become more and more important. This inelastic contribution to the Glauber corrections can be determined by our measurements. They are important for the Glauber theory itself and also as a source of information on inelastic processes.

From the p-d elastic scattering we can also deduce information about p-n scattering.[13]

C. Inelastic Scattering

The production of isobars having masses of 1236, 1400, 1520, 1688, and 2190 MeV in p-p reactions has been investigated quite extensively up to $|t| = 6$ $(GeV/c)^2$ and $P = 24$ GeV/c.[14] These results show that the differential cross sections for the 1520, 1688, and 2190 isobars have relatively small slope parameters ($b = 3 \sim 5$) and that they are comparable to that for elastic scattering around $|t| = 1$ $(GeV/c)^2$ as shown in Fig. 5. Moreover, the cross sections for producing these isobars are roughly s-independent up to $P = 24$ GeV/c.

At momenta less than 24 GeV/c where the bulk of data on isobars exists, both elastic and inelastic cross sections have a

break at $|t| \sim 1.4$ $(GeV/c)^2$, as shown in Fig. 5. It is known that at larger s this kink becomes a dip for elastic scattering. It will be extremely interesting to learn also what happens to isobars.

As shown in Fig. 9, our mass resolution on the recoil particle using only the recoil arm is good enough to separate the isobars at 200 GeV beam energy for $0.2 \lesssim |t| \lesssim 10$ $(GeV/c)^2$. At higher beam energies the separation of isobars becomes more difficult, especially between the 1520 and 1688 isobars. Thus, we expect to measure isobar production cross sections certainly at 200 GeV and perhaps up to 400 GeV in incident energy.

The diffractive excitation of large masses is a very interesting phenomena discovered experimentally within the last few years.[15] We will be able to measure the excitations of masses up to $M_X \approx 20$ GeV and check scaling hypotheses and the predictions of different theoretical models.

There is a fundamental reason for interest in inelastic scattering on deuterium and other nuclei[16] because here one has the possibility to investigate the space-time development of hadronic processes. In the case of isobar excitation we can measure the isobar-nucleon interaction, which is impossible in ordinary hadron-hadron reactions.

Recent measurements from the ISR and NAL show that the inclusive cross section for hadron production at large transverse momentum is much larger than expected from an exponential extrapolation of small p_t data.[17] It is commonly believed that collisions at large p_t reflect the properties of basic interactions

at short distances. With our spectrometer we can investigate the s- and p_t- dependence of differential cross sections over a wide range.

III. EXPERIMENTAL SETUP

The angles and momenta of recoiling particles are measured by a magnetic spectrometer using proportional chambers. At higher beam energies and near the extremes of the t-region we wish to study, the resolution of the recoil spectrometer alone is insufficient to give a clean separation of elastic and inelastic scattering. Thus, it will be necessary to use at least a forward hodoscope in order to give a clean separation between elastic and inelastic scattering. In Phase I of this experiment a hodoscope will be placed in the forward direction to measure the angles of forward scattered particles; in Phase II a forward magnetic spectrometer will be used to measure both the momenta and angles of the forward particles.

A. Recoil Particle Spectrometer

We propose to make a magnetic spectrometer with two bending magnets and a wire proportional chamber system to measure the momenta and angles of recoil particles. In Fig. 6 this recoil spectrometer is shown in one of the tentative versions of the expanded C0 internal target laboratory. This spectrometer subtends about 0.94 msr with a polar angle coverage of about 2.8° in the laboratory system. Its resolution is sufficient for the measurements of p-p and p-d elastic and inelastic scattering over a wide range in t without the use of a forward hodoscope or momentum spectrometer.

The spectrometer consists of two bending magnets, four vertical proportional chamber planes, two horizontal proportional chamber planes, Cerenkov counters, and scintillation counters. The relative position of these components to the target and beam line is also shown in Fig. 6. The system is mounted on a carriage which may be rotated remotely about the jet target.

The first two wire proportional chamber planes, W1 and W2, with vertical wires spaced at 1 mm, define the recoil angles to an accuracy of about ±0.1 mrad. The recoil particle trajectory will be extrapolated back to the target to check that it originated in the target.

There is a chamber, W3, between the two magnets, and another similar chamber, W4, 4.5 meters downstream from the second magnet. These chambers have one millimeter wire spacing vertically and

two millimeters spacing horizontally. Between wire chambers we will install vacuum chambers to reduce multiple scattering.

One possible design of a recoil spectrometer bending magnet is shown in Fig. 7. This is almost a C-shaped magnet having only a thin yoke on the beam side. We plan to operate these magnets at 18 kilogauss. With this field 2.9 and 6.3 GeV/c protons, corresponding to $|t| = 4$ and 10 $(GeV/c)^2$, will be bent in the horizontal plane by 32.1° and 14.7° respectively. The momentum resolution, $\Delta p/p$, will be about 0.05% and 0.063% respectively. Also, we are considering the use of two superconducting magnets (24-8-72), which are being developed in the Research Division, if they are available to us. As there is already a He liquefier in C0 area, the operation of these superconducting magnets must be easily started here.

The solid angle defining counter S1 is at the end of the spectrometer as is a second scintillation counter, S2. An absorber and a Cerenkov counter are placed between them. A signal derived from the coincidence of S1 and S2 will be used to register events into the computer. In addition, a coincidence is required with the RF structure of the main ring beam to avoid events not originating in the target. Pulse height in the Cerenkov counter will be recorded and used to help eliminate background due to pions.

Time of flight will be used at low t values. The time of flight difference at 2.9 GeV/c for pions and protons ($|t| = 4 (GeV/c)^2$) is about 2 ns. At larger momentum transfers (such that laboratory recoil momentum = 2.5 - 6 GeV/c) a gas Cerenkov counter will be used to discriminate between protons and pions.

The p-p and p-d elastic scattering kinematics are shown in Fig. 8 for 300 GeV incident energy. At large fixed angles, the t-value of elastic scattering changes very little for incident energies from 100 to 500 GeV. The spectrometer, set at recoil angles between 30° to 90°, will cover the t-region of interest at different incident energies.

B. Mass Resolutions

Measuring only the recoil proton, the missing mass squared of the forward scattered particle is given by

$$M^2 = m_o^2 + 2m_r^2 + 2m_r (E_o - E_r) - 2(E_o E_r - p_o p_r \cos\theta_r).$$

Here the subscripts o and r refer to the incident and recoil particles respectively. Thus, the missing mass resolution can be estimated by taking

$$\Delta M^2 = \left[\left(\frac{\partial M^2}{\partial p_o}\right)^2 (\Delta p_o)^2 + \left(\frac{\partial M^2}{\partial p_r}\right)^2 (\Delta p_r)^2 + \left(\frac{\partial M^2}{\partial \theta_r}\right)^2 (\Delta \theta_r)^2\right]^{1/2}.$$

The results of our calculations are shown in Fig.9A for p-p elastic scattering and Fig.9B for p-d elastic scattering. We have taken into account multiple scattering in the vacuum chamber windows and proportional chambers and also the position measurement error in the chambers. The rise in ΔM^2 at low t is due to an increase in multiple scattering while at higher t the rise is due to the momentum resolution.

Figure 9A shows that the resolution of the recoil spectrometer alone is sufficient to give a good separation between elastic and inelastic scattering. If, for example we take $\Delta M^2 \lesssim 0.6\ (\text{GeV})^2$

($\Delta M \simeq 0.32$ GeV) as the mass resolution necessary to separate the elastics from $N^*(1470)$, from the standpoint of resolution only we can measure from $t = 0.1, 0.25$, and 1.1 $(GeV/c)^2$ at incident energies of 100, 300, and 500 GeV respectively.

Of course, the use of a forward hodoscope (Phase I) or forward magnetic spectrometer (Phase II) will make the separation between elastics and inelastics cleaner by allowing the use of coplanarity and elasticity constraints. Because we cannot move the forward hodoscope arbitrarily close to the beam there is an acceptance cutoff in $|t|$ beyond which we cannot use the forward system for measuring lower values of $|t|$. For example, this cutoff occurs at $|t| = 0.14$, and 0.4 $(GeV/c)^2$ for incident beam energies of 300 and 500 GeV respectively.

C. Forward Hodoscope (Phase I)

In Phase I a scintillation counter hodoscope will be placed in the forward arm so as to allow the imposition of coplanarity and opening angle constraints. This hodoscope would be placed 40m from the jet target.

At 400 GeV/c the forward proton from the decay of the 1400 MeV N^* is allowed within a cone of $\sim$1mr away from the N^* direction. In order to reduce the background from these events we should have angular resolution at least 10 times better than this cone angle, or $\sim$0.1 mr. This implies hodoscope elements whose dimension is $\sim$0.4 cm. We will accomplish this with 30 counters 0.8 cm wide with half overlap giving 29 bins of $\sim$0.1 mr and $\sim$3 mr for the forward particle.

Several counters following this hodoscope will cover the

azimuthal bite of the recoil spectrometer while accepting only ~0.1 mr in the dip angle.

D. Forward Particle Spectrometer (Phase II)

As is shown in Fig. 10, the forward scattered particles at fixed angle have increasing momentum and t-values as the circulating beam energy increases. Therefore, the system at a fixed position with a fixed current measures elastic scattering for one energy only. The laboratory angle for the forward scattered particle at $|t| = 4$ $(GeV/c)^2$ is 6.9, 5.2, and 4 mr for 300, 400, and 500 GeV beams respectively.

The system consists of three bending magnets and four sets of scintillation counter hodoscopes. At 300 GeV the front end of the first magnet is placed 19.1 meters downstream from the jet target in order to cover the t-region from 4 to 10 $(GeV/c)^2$. The current in the magnets as well as the position and angles of the magnets will be adjusted to accept only the elastically scattered protons. The momentum acceptance, which should be about 0.5%, can be easily achieved and the necessary horizontal acceptance is 2 mr. The solid angle is defined by the recoil spectrometer.

The scintillation counter hodoscopes are before the first magnet, between magnets, and after the last magnet in the forward spectrometer. There are also some anticoincidence counters to veto particles scattered from the steel surface and from the outside. With the information from the forward spectrometer the coplanarity and elasticity of the events will be determined, and we can select the elastically scattered protons from the background.

If necessary, proportional chambers will be installed near the end of the forward spectrometer to improve resolution. For completeness we show the layout of the forward spectrometer for a different energy in Fig. 11.

The magnets are similar to the main ring magnets as far as aperture and length are concerned. The steel core is shaped like the recoil spectrometer, as shown in Fig. 7B. The outside dimensions will be about 28 inches high and 27 inches wide.

The first magnet has an aperture 1.5 inches high and 9.75 inches wide with a 16 turn coil. The inside yoke is 1/4 inch thick and the coil is 2.39 inches wide. Therefore, the particle can go through the magnet at a minimum distance of 2.64 inches from the outside surface. The second and third magnets have an aperture 2.0 inches high and 8.73 inches wide and 24 turn coils.

These magnets are connected in series and are excited by the same power supply to a magnetic field of about 18 kG with 3500 Amp. The resistance of the first and second magnets will be about 17 and 26 m Ω. The maximum total power consumption for these three magnets will be about 850 kW. These are conventional magnets, but they could be made with superconducting wire to save power.

The main ring vacuum pipe at C0 will be shifted outward by one inch relative to the center line connecting the upstream and downstream quadrupole magnets. The injected beam will be centered in this pipe with local low field correction magnets. However, the high energy beam will be set to run 2 inches from the inner surface of the 6 inch pipe as shown in Fig. 7B. As the extraction

septum in A0 is set at 3 cm outside the center line and the abort target in D0 is set at 1.5 inches, this would not seem to be a problem.

The use of a local magnetic field beam bump at high energy will be considered. With this modification the beam will be shifted inward to make a lower t-region accessible in the coincidence experiment.

E. Monitor

We will install a vacuum guide at right angle to the main ring beam line, which is about 5 meters long and covers laboratory angles roughly from 90 to 80 degrees. At the end of it will be installed solid state detectors which will be used to monitor small angle elastic events.

An experimental setup and procedure similar to those of Experiment #36 and 186 will be used, except with better precision for the measurement of the Coulomb interference region. The setup is shown in Fig. 6B.

We will use 6 discrete solid state detectors in the t-range from 0.02 to 0.15 $(GeV/c)^2$ and 6 detectors in the t-range from 0.001 to 0.02 $(GeV/c)^2$. Electronics which are similar to those used for Experiment #36 or #186 will be employed. The experimental procedure is quite established now. The measured shape of $d\sigma/dt$ around the Coulomb-nuclear interference region is shown in Fig. 12.

As an option we may consider using position sensitive detectors, which give energy and position information at the same time for each event. Some of the data from Experiment #36 was taken with such detectors and is now being processed. The position sensitive

detectors were developed in the last few years, and will give a spatial resolution of better than 0.5 mm over their 5 cm width.

IV. COUNTING RATES

The counting rate, N, per jet pulse is given by the following equation:

$$N = N_b N_t \frac{d\sigma}{dt} \Delta t \frac{\Delta\phi}{2\pi}$$

where N_b is the number of circulating protons available during a pulse of the jet and N_t is the number of target particles. The azimuthal acceptance, $\Delta\phi$, and the t-acceptance, Δt, are determined by the recoil spectrometer since the forward hodoscope (Phase I) and forward spectrometer (Phase II) are large enough to accommodate all forward particles from elastic scattering events which are detected by the recoil spectrometer. Using estimated $d\sigma/dt$ values from presently available data, N is given in Table 3.

The present density of the jet is about 5×10^{-7} g/cm^3 in a beam interaction region of about 1 cm, giving $N_t = 3 \times 10^{17}$ proton/cm^2 available as our target. Within a main ring cycle the jet duration is about 200 ms, and 3 or 4 jet pulses in a main ring cycle are possible. For the lower t-values we plan to operate the jet during the ramp and for higher t-values we may use the flat-top or front porches of the main ring ramp.

The presently available beam intensity in the main ring is about 4×10^{12} protons/pulse, which should eventually increase to the design intensity of 5×10^{13} proton/pulse. For these calculations we have assumed 1×10^{13} protons/pulse which may be a conservative value in the latter part of 1974. During a 200 ms

jet pulse the main ring beam circulates 10^4 turns around the ring, giving an available beam during a jet pulse $N_b = 10^4 \times 10^{13} = 10^{17}$ proton/pulse. We plan to operate at least one jet at low energy and another at higher energy for which the forward hodoscope or spectrometer is adjusted. When feasible, we will operate 2 or 3 jets, during flat-top.

It is possible that the counting rates listed in Table 3 can be increased by a factor of 50 in the near future with increases in the jet density and beam intensity. The Russian members of our collaboration are presently exploring the possibility of increasing the jet density by reducing the jet velocity and using solid hydrogen or deuterium. With such modifications the jet density may be increased by a factor of 10 or more. This, coupled with an increase in beam intensity to 5×10^{13} proton/pulse, could increase our listed counting rates by a factor of 50 or more in the near future.

V. BACKGROUND RATES

There are two types of background: one target associated and the other not. The background which does not come from the target was measured in May 1973 at 300 GeV to be about 16 minimum ionizing particles/cm^2/sec/10^{10} circulating protons at 3.5 feet from the beam line.[18] Thus, at 13 cm from the beam line and with 10^{13} circulating protons, the corresponding number is 1.3×10^5 particles/cm^2/sec. Although this rate is tolerable for the forward hodoscope, it will be reduced by at least an order of magnitude. First of all, the experimental area at C-0 will be designed more carefully so as not to restrict the circulating beam. Secondly,

a beam scraper at A17 and beam collimators at D-0 will be used, if needed.

The effect of the accidental rate due to particles coming from the target can be estimated for the forward spectrometer including the first forward hodoscope as follows. This hodoscope is more seriously affected than the recoil spectrometer. We estimate the background rate at the $|t| = 4$ $(GeV/c)^2$ setting at 300 GeV. As there is a maximum of 1113 beam bunches in the main ring, we have $N_b = 10^{10}$ proton/bunch for a beam intensity of 10^{13} ppp. The interval between beam bunches is about 20 ns and the total number of reactions during a bunch is estimated from a total cross section of 40 mb as follows:

$$N_b N_t \sigma_{tot} = 10^{10} \times 3 \times 10^{17} \times 40 \times 10^{-27} = 120$$

The multiplicity measured by the bubble chamber is about 8.9 at 303 GeV, and the projected distribution in one dimension is shown in Fig. 13, where the events are grouped in 0.5 mr bins.[19] Therefore, we have about 1000 charged particles coming from a jet target associated with a single beam bunch. The maximum number of particles going through the aperture of the first useful magnet opening (which is 4 mr horizontally and 1.5 inches high) is estimated to be less than 0.6%. Thus, on the average, six particles may go through this opening; we can easily select the elastic scattered proton from the information given by the following counter hodoscopes. As these 1000 charged particles may produce many low energy daughter particles when they finally hit vacuum chambers and magnets, it is preferable to use a thin vacuum tube and also to place the counter hodoscope so that the back scattered particles reach the hodoscope out of phase with the

scattered particles of interest, e.g., 10 ns later. The number of muons was measured in the C0 area by Experiment #120.[20] They observed 500 μ/jet (=200 ms)/10^{12} proton at 250 GeV with a counter of 2/3" x 2/3" placed at 16 mr and at 32 feet downstream from the jet. This gives 2.5 x 10^{-3}/bunch (=20 ns)/10^{13} proton/2 msr at 16 mr. This number will not cause difficulty for this experiment.

VI. COMPARISONS WITH OTHER EXPERIMENTS

A. Advantages of Internal Target Area

In the future, elastic scattering will be measured at NAL using external beams. However, we can measure the elastic and inelastic scattering of p-p and p-d in the main ring in a very flexible and efficient way. There are several advantages of the internal target experiment over external target experiments for these reasons:

1. It is possible to select the incident beam energy freely from the injection energy to the highest extraction energy. Thus, the s-dependence measurement can be done easily and in a bias free way.
2. The internal target has the first access to the highest machine energy, because no external beam line is needed. When the energy doubler becomes operational, this experiment will have immediate access to this new energy without awaiting a new beam transport system.
3. The target is thin, so that the multiple scattering of the recoil particle is small compared to that of a liquid hydrogen target. Therefore, elastic scattering may be measured using only the recoil spectrometer over a large

range of t (see Fig. 9).

4. For the same reason as in 3, the mass resolution is much better than in experiments using regular hydrogen targets. Thus, the isobars can be easily studied.
5. The luminosity for the internal target is comparable to that of the external beam. For the internal target with three pulses of 200 ms width and a beam intensity of 10^{13} ppp, $L = N_b N_t = 10^{13} \times 3 \times 10^4 \times 5 \times 10^{-7} \times 6 \times 10^{23} = 0.9 \times 10^{35}$. For the external beam with 4×10^{11} ppp and 4" long liquid hydrogen target we have:

$$L = N_b N_t = 4 \times 10^{11} \times 4 \times 2.54 \times 0.071 \times 6 \times 10^{23} = 1.7 \times 10^{35}.$$

6. At the internal target the incident beam has no halo and no pion contamination; identification of incident particles using Cerenkov counter is therefore not necessary.
7. This experiment can be done parasitically with respect to external experiments. Therefore there is always more machine time available.
8. Power consumed by this experiment is minimal since no external beam line is required.

B. How Do these Unique Features Translate into a Better Experiment?

Because of the items mentioned above it is possible to design a recoil spectrometer which has sufficient resolution to separate elastics and diffractively produced N^*'s up to large values of t (e.g., at 300 GeV our design is fully capable of these measurements up to 10 $(GeV/c)^2$).

Because of this resolution it is possible in the internal target area to cover the t range from 0.2 to 10 $(GeV/c)^2$ with one experiment, whereas such a capability is not presently available in the approved experiments. Hence, the attendant relative normalization difficulties encountered when attempting to compare different experiments is no longer a problem.

This is truly a unique feature in that all other presently approved experiments (except E-96) require double arm capability in order to isolate elastic scattering. Single arm mass resolution alone is insufficient, and hence the inelastic spectrum is not studied well by these experiments. In the case of E-96 the t region covered is out to $\sim$1.5 $(GeV/c)^2$ and the highest beam energy at which elastic scattering may be studied is $\sim$200 GeV/c.

We cannot overemphasize the importance of having all energies simultaneously available. Many of the important questions in high energy pp scattering require measurement of a slowly varying energy dependence. The internal target laboratory is ideal for such measurements. The kinematics of the recoil particle vary only slowly as the incident momentum is varied, thus making systematic error minimal. The hydrogen jet may be pulsed several times during the ramp. Thus, in one machine cycle, data at several energies may be accumulated. The relative normalization of the various energies is thus made much more reliable than when these data must be accumulated during peirods which may be separated by days. We believe this feature of our experiment to be very important when the energy dependence sought can be as

slow as logarithmic.

Finally, it is worthy of note that all this is accomplished with what is essentially a simple apparatus requiring detection of particles only up to 6 GeV/c in the recoil arm. The simplicity of the apparatus, in our view, will tend to make the apparatus reliable, stable, and easy to understand; the data will hopefully also have these same properties.

C. Summary of Relevant Experiments:

1. Exp. 7 Summary

This experiment measures elastic scattering of π, K and p up to 200 GeV/c and out to t-values of $\sim$3 $(\text{GeV/c})^2$. The low lying N^*'s may be accessible with only the forward spectrometer up to incident energies of $\sim$80 GeV/c.

2. Exp. 63 Summary

This experiment is primarily a particle production survey detecting particles with lab momentum <2.4 GeV/c for incident protons in the 50-500 GeV/c range. Elastic scattering is not emphasized; however, we may assume that this experiment has access to elastic pp scattering out to t $\sim$1.5 $(\text{GeV/c})^2$.

3. Exp. 96 Summary

The high resolution--high momentum spectrometer in the meson area will be used to study elastic $K^{\pm}$, p, and $\bar{p}$ scattering from protons and deuterons. The incident momentum accessible is from 50 to 200 GeV/c while the t-range accessible is up to $\sim$1.5 $(\text{GeV/c})^2$. In addition, the inelastic spectrum will be studied up to $M_x \lesssim 2$ GeV.

4. Exp. 177 Summary

pp elastic scattering will be measured at 200 and 400 GeV. A double arm spectrometer is employed to measure the differential cross section for t-values between 4 and 20 $(GeV/c)^2$.

5. Exp. 231 (this proposal) Summary

pp and pd elastic will be measured for beam energies between 8 and 500 GeV. These measurements will cover the t-region from 0.2 to 10 $(GeV/c)^2$ for pp elastic scattering and 0.2 to 5 $(GeV/c)^2$ for pd elastic scattering. In addition, the single arm resolution is sufficient to measure diffractively produced N^*'s to large t-values also. This capability does not presently exist in the above approved experiments.

VII. APPARATUS

We are assuming the construction of the C0 internal target area will be started in the spring of 1974. Allowing six months for construction of this area, we expect the experimental area will be ready for occupation in the fall of 1974. While the experimental area of the C0 straight section and the service building are under construction, we will work on preparations for the experiment.

The major items which are needed for the experiment are:

1. Jet target and its control system
2. Recoil spectrometer magnets
3. Forward spectrometer magnets (Phase II)

4. Power supplies for spectrometers
5. Cooling system for spectrometers
6. Fast logic circuits
7. Proportional chamber system including Camac and its interface
8. Scintillation counter hodoscopes
9. On-line PDP-11 system
10. Solid state detector monitor system
11. Cerenkov counters

Dubna will supply the jet target and its control system. We request NAL to supply the spectrometer magnets and power supplies as well as the cooling system. Two superconducting magnets (24-8-72) may be available as recoil spectrometer magnets. Purdue University will build the proportional chambers, Cerenkov counters and all scintillation counters. NAL will supply fast logic circuits, the readout electronics for the chambers, the PDP-11, and Camac and its interface. Dubna will provide electronics for the monitor system.

VIII. EXPERIMENTAL PROCEDURE

We think we can build or have all the experimental equipment except the forward spectrometer magnets in six months. The existing superconducting magnets (24-8-72) may be available as recoil spectrometer magnets. Therefore, we can start Phase I of this experiment without any trouble.

In Phase I we will study p-p and p-d elastic and inelastic scattering in the lower t-region up to 5 $(GeV/c)^2$ with continuous incident energies using only the recoil arm and forward counter hodoscope. For this phase of the experiment we need about 400

hours of running time.

In the Phase II, using both the forward and recoil spectrometers, we will measure p-p elastic scattering in the high t-region with 200, 300, 400, and possibly 500 GeV beams. This experiment needs about 600 hours of running.

Thus, we are requesting a total of 1,000 hours of running time for all experiments. Within one month after we move into the new area, we will be able to start the experiment. Members of our collaboration started the C0 Internal Target Area and also helped carry out other experiments. This has provided a driving force in C0 and we expect to provide a similar driving force in the new C0 Internal Target Area.

IX. POSSIBLE FUTURE EXPERIMENTS

The elastic scattering experiment we propose to do should be the first experiment in the new Internal Target Area; it will provide data essential to understanding the apparatus for further experiments. Using the same equipment and with some modifications the apparatus can also do the following experiments.

A. $p+p \rightarrow \bar{p}$ + Anything

This can be investigated by changing the polarity of the recoil magnets.

B. $p+p \rightarrow \pi^{\pm}$ + Anything

These two reactions will be very interesting to study over the entire s-range. We can do these experiments using the proposed Cerenkov counters in the recoil arm to identify pions.

C. Elastic Scattering from Some Nuclei

Elastic scattering from some nuclei can be measured using the same equipment by observing the recoil nuclei with the low momentum spectrometer.

D. Polarization Measurement

A carbon polarizer can be placed after the first magnet of the recoil spectrometer in order to measure the left-right assymmetry with use of an extra set of wire chambers. A polarization measurement in the region around the dip at $|t| = 1.3$ $(GeV/c)^2$ should help provide an understanding of the mechanism responsible for the dip.

E. $p+p \rightarrow \pi^+ + d$

F. Particle Production Experiment

Using the recoil spectrometer and adding Cerenkov counters, we can measure the production rate of $\pi^{\pm}$, $K^{\pm}$, and other particles at large angles.

G. pp Total Cross Section up to 500 GeV

Using solid state detectors, we can measure the pp total cross section with an accuracy of $\pm$ 0.5 mb.

H. Fine Oscillatroy Behavior in the pp Elastic Scattering Differential Cross Section

Recently a fine oscillatory structure in the pp elastic scattering differential cross section below $|t| = 0.2$ $(GeV/c)^2$ was suggested.[21] This behavior can be investigated by using the solid state detectors.

X. MANPOWER

In addition to the physicists listed on the title page, we expect one or more people from NAL and at least one graduate student from Purdue University to join the experiment when it is approved.

XI. NEW C0 EXPERIMENTAL AREA

In order to cover the t-region discussed in the text, we feel that the new C0 experimental area should have the following features:

1. The recoil spectrometer area should allow the spectrometer to cover from 90° to 30° with respect to the beam direction.
2. The allowable radial length of the recoil spectrometer should be greater than 15 meters.
3. The recoil spectrometer area should be placed near the upstream end of the C0 straight section. If this is not the case, we will be limited in t range at 500 GeV.

APPENDIX

The Difference between the Old Concept of an Internal Target Laboratory and the Internal Target Area Using Jet Target.

The present and planned Internal Target Area is quite different in nature from what was conceived as an Internal Target Laboratory six years ago as a general facility. With the invention of the gas jet target at Dubna and with subsequent very successful experiments at the Dubna and Serpukhov accelerators, the Internal Target Area of NAL was started two years ago and already many experiments have been finished.

In the old conception, we were going to use a solid beryllium target or some other material as an internal target to make a diffractively scattered proton beam and secondary particle beams in the main ring. Subsequently these beams might have been extracted. In this conception, we would have used as much equipment as needed for an extraction system in the transfer hall and a much more complicated control system might have been required. As we would have to use a solid target, the radiation loss might have been very heavy and the operation of this area might have been very complicated, and it might have affected the operation of the synchrotron tremendously. Also many downstream main ring magnets might have been exposed to scattered particles and made highly radioactive.

In the present internal target area we have been doing experiments using the jet as a target without interacting with the circulating beam too much. Only one tenth of a percent or less of the circulating beam intensity is lost. The operation is fairly simple and we do not detect any noticeably high radiation

effects on downstream magnets. The interaction with the operation of synchrotron has been minimal.

Yet four experiments have been finished and another four experiments are going on now. There are already several published papers on the slope parameter b and the ratio α of the real part to imaginary part of the scattering amplitude for p-p elastic scattering on the pp $\rightarrow$ pX inclusive reaction, and on the γ spectrum from pp and p-nucleus reactions.

The present internal target area has been very useful and fruitful for studying high energy physics in the early stages of the NAL accelerator. We think the usability of this area will be much enhanced by the addition of the extended internal target area.

REFERENCES

[1] D. Jovanovic et al., 1973 NAL Summer Study Report, in Press.

[2] V. Bartenev et al., Phys. Rev. Lett., 31, 1088 (1973).

[3] V. Bartenev et al., Phys. Rev. Lett., 31, 1367 (1973).

[4] V. Bartenev et al., "Diffraction Excitation of Nucleon Resonances in p-p Collisions at Incident Proton Energies from 175 to 400 GeV/c", paper submitted to APS Division of Particles and Fields Meeting, Berkeley, August, 1973.

[5] F. Sannes et al., Phys. Rev. Lett., 30, 766 (1973).

[6] D. C. Carey et al., Phys. Rev. Lett., 32, 24 (1974).

[7] U. Amaldi, CERN NP Internal Report 73-5, April 1973.

[8] L. Durand III and R. Lipes, Phys. Rev. Lett., 20, 637 (1968).
T. T. Chou and C. N. Yang, Phys. Rev. Lett., 20, 1213 (1968).

[9] R. J. N. Phillips and V. Barger, Phys. Lett., 46B, 412 (1973).

[10] E. Malamud and W. Pelczarski, Proposal for a New Internal Target Hall. NAL Internal Report (1973).

[11] F. Bradamante et al., Phys. Letters 32B, 303 (1970).
U. Amaldi et al., Nuclear Physics B39, 39 (1972).

[12] V. Franco and R. J. Glauber, Phys. Rev. Lett., 22, 370 (1969).

[13] U. Amaldi et al., Nuclear Physics B39, 39 (1972).
G. G. Beznogikh et al., Dubna Preprint E1-7215 (1973).

[14] J. V. Allaby et al., Nuclear Physics B52, 316 (1973).

[15] D.W.G.S. Leith, SLAC-PUB-1330 (1973).

[16] K. Gottfried, CERN Preprint TH1735.

[17] J.K. Walker, NAL-Conf-73/67-THY/EXP (1973).
J.W. Cronin et al., Phys. Rev. Lett., 31, 1426 (1973).

[18] J. Johnson. Private communication.

[19] J. Schivell. Private communication.

[20] R. Imlay. Private communication.

[21] V. A. Tsarev, NAL-Pub-74/17 THY/EXP (1974).

Table 1 - pp Elastic Scattering (at 300 GeV/c)

	t range	Recoil Proton P (GeV/c)	E (GeV)	Angle (°)	Scattered Proton P (GeV/c)	Angle (°)	Physics
1.	$0<t<0.01$	$P<0.1$	$E<0.005$	$\theta>87$	$=300$	<0.02	Coulomb Interference Real Part
2.	$0.01<t<0.2$	$P<0.46$	$E<0.11$	$\theta>76.5$	$=300$	<0.09	Break in b Fine oscillation
3.	$0.2<t<1$	$P<1.2$	$E<0.55$	$\theta>61.5$	>299.5	<0.19	
4.	$1<t<10$	$P<6.2$	$E<5.4$	$\theta>42$	>294.6	<0.61	Dips
5.	$10<t<100$	$P<54.3$	$E<53.3$	$\theta>9.6$	>246.5	<2.1	
6.	$100<t$						

Table 2 - pd Elastic Scattering (at 300 GeV/c)

	t range	Recoil Deuteron P (GeV/c)	E (GeV)	Angle (°)	Scattered Proton P (GeV/c)	Angle (°)	Physics
1.	$0<t<0.01$	$P<0.1$	$E<0.003$	$\theta>88.5$	$=300$	<0.02	Coulomb Interference Real Part
2.	$0.01<t<0.2$	$P<0.45$	$E<0.053$	$\theta>83.2$	$=300$	<0.09	Single Scattering
3.	$0.2<t<1$	$P<1.0$	$E<0.27$	$\theta>75$	>299.7	<0.19	Interference between single and double scattering
4.	$1<t<10$	$P<4.2$	$E<2.7$	$\theta>50$	>297.3	<0.61	Double scattering
5.	$10<t<100$	$P<28.4$	$E<26.6$	$\theta>19.6$	>293.4	<2.0	
6.	$100<t$						

TABLE 3

Calculated Counting Rates for Experiment 231

We have assumed a jet density of 5×10^{-7} gm/cm^3, a 200 msec jet pulse, and a 1 cm interaction region.

	$\lvert t\rvert$ (GeV/c)^2	$\frac{d\sigma}{dt}$ [cm^2/(GeV/c)^2]	Δt (GeV/c)^2	θ (Degrees)	$\Delta\varphi$ (Radians)	No. of Events / Jet Pulse	No. of Events / day
pp Elastic Scattering	1	1.5×10^{-30}	0.24	61.7	0.022	37.1	1.28×10^{6}
	2	4×10^{-32}	0.41	52.8	0.024	1.90	6.55×10^{4}
	4	3×10^{-33}	0.78	42.9	0.028	0.32	1.10×10^{4}
	10*	$\sim 1\times10^{-36}$	4.0	30.3	0.05	0.001	33
pd Elastic Scattering	1	6×10^{-30}	0.39	74.9	0.020	223	7.7×10^{6}
	2	1×10^{-31}	0.56	69.1	0.021	5.52	1.91×10^{5}
	4*	$\sim 5\times10^{-35}$	1.7	61.5	0.028	0.01	3.9×10^{2}

*Phase II, where the recoil spectrometer is moved up to 2.5 meters from the target.

LIST OF FIGURES

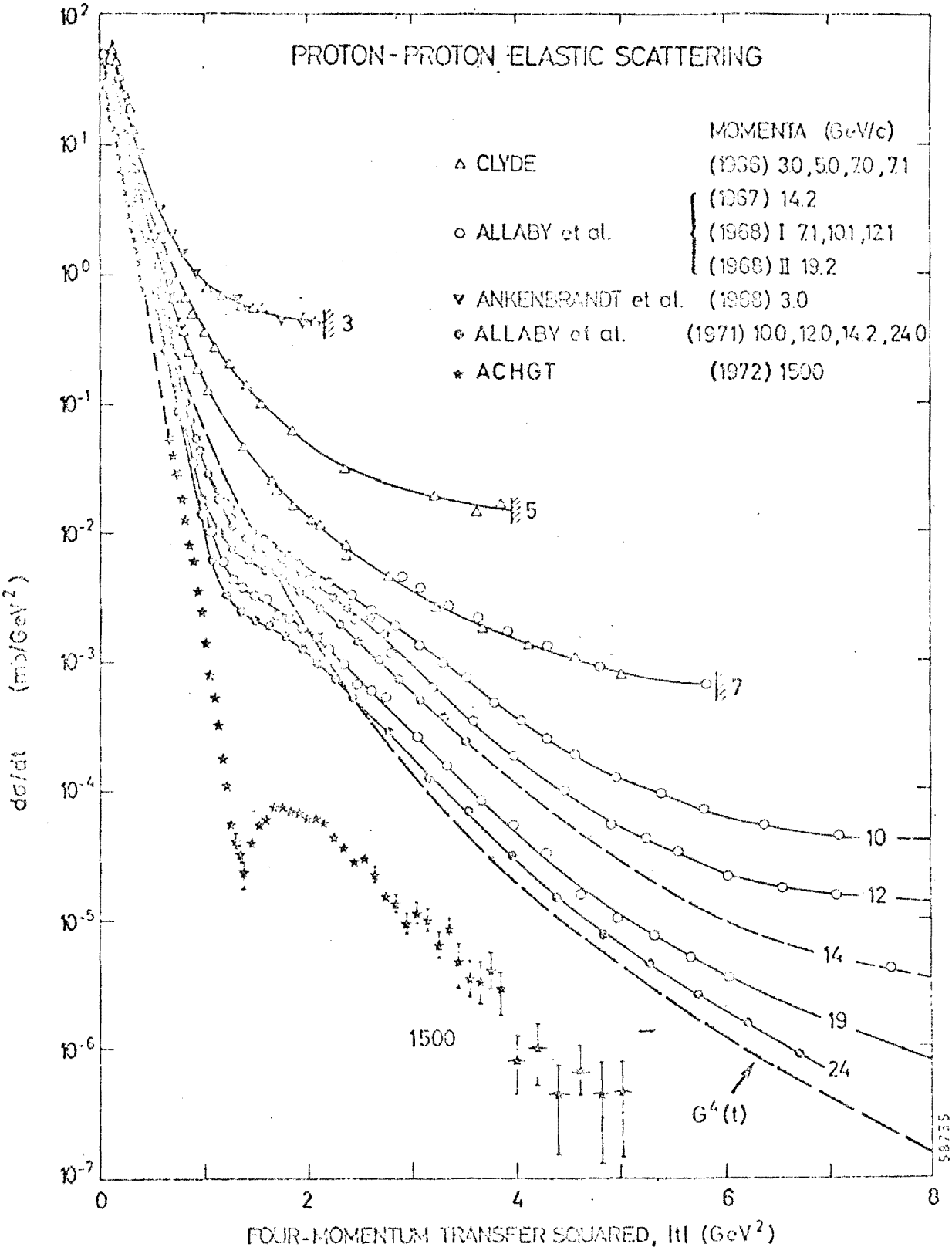

Fig. 1 Proton-Proton Elastic Scattering

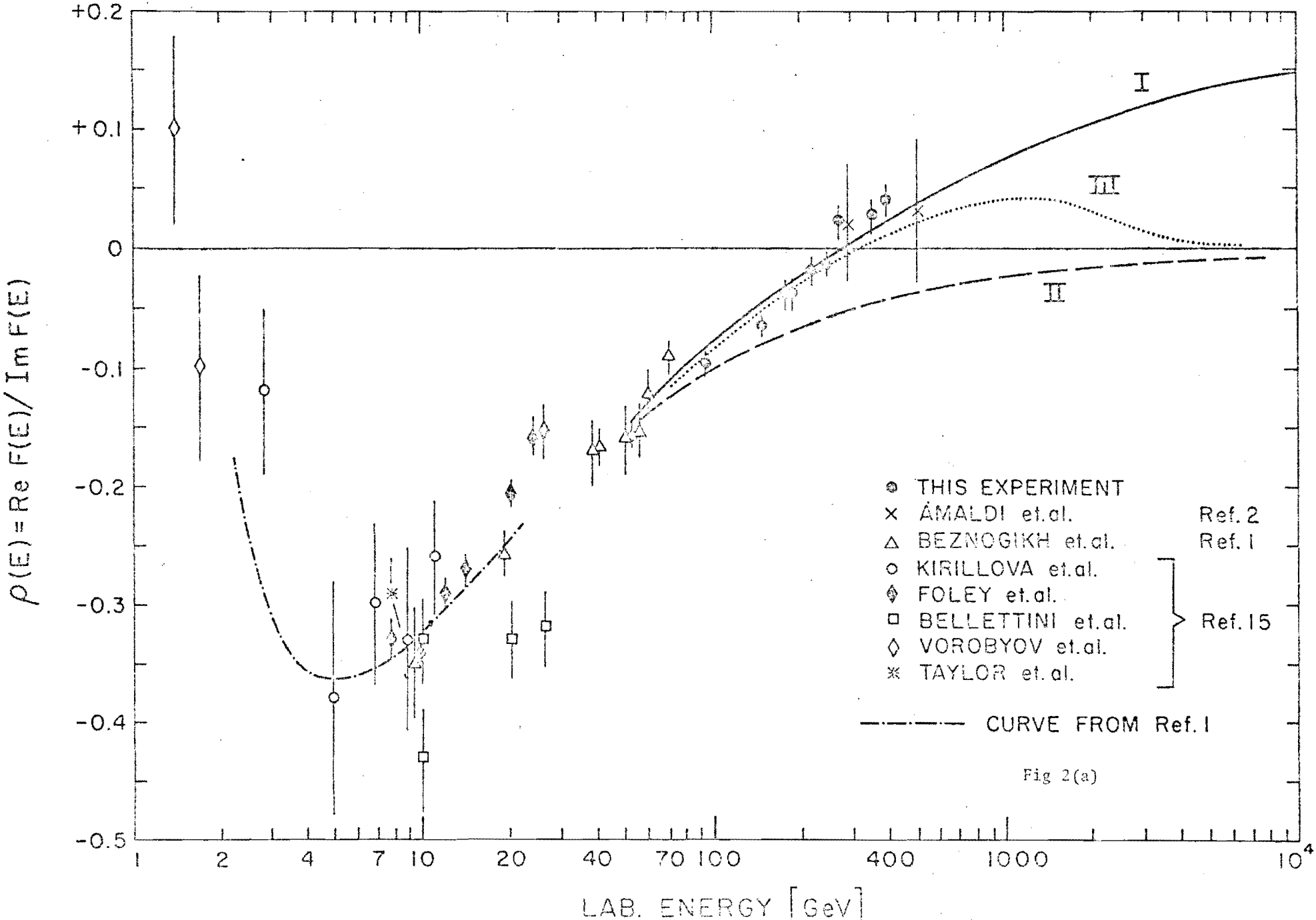

Fig. 2. Ratio of Real Part to Imaginary Part of Scattering Amplitude.

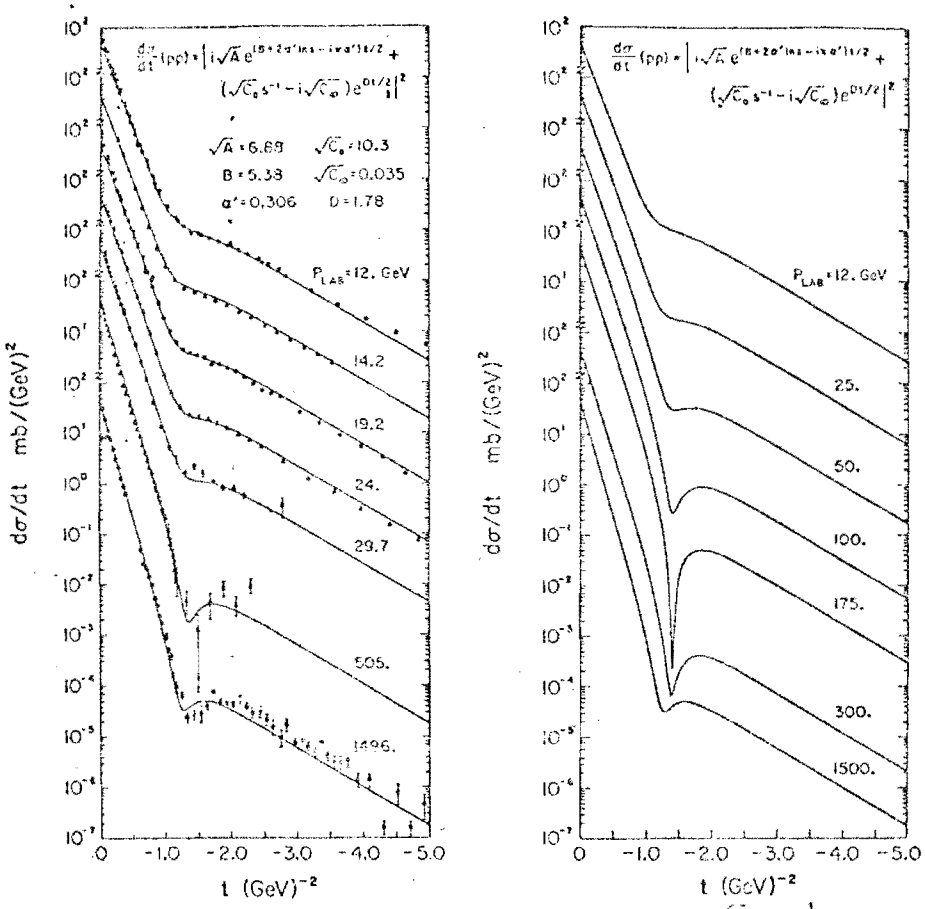

Fig. 2. Description of the pp data for $0.15 < |t| < 5.0$ with the parametrization $d\sigma/dt = |i\sqrt{A}\exp(\frac{1}{2}B + \alpha' \ln s - i\alpha'\pi/2)t + (\sqrt{C_0}\, s^{-1} - i\sqrt{C_\infty}\exp(\frac{1}{2}Dt)|^2$. Predictions at intermediate momenta are also illustrated.

Fig. 3. Differential Cross Section Prediction for Proton-Proton Elastic Scattering by Phillips and Barger.

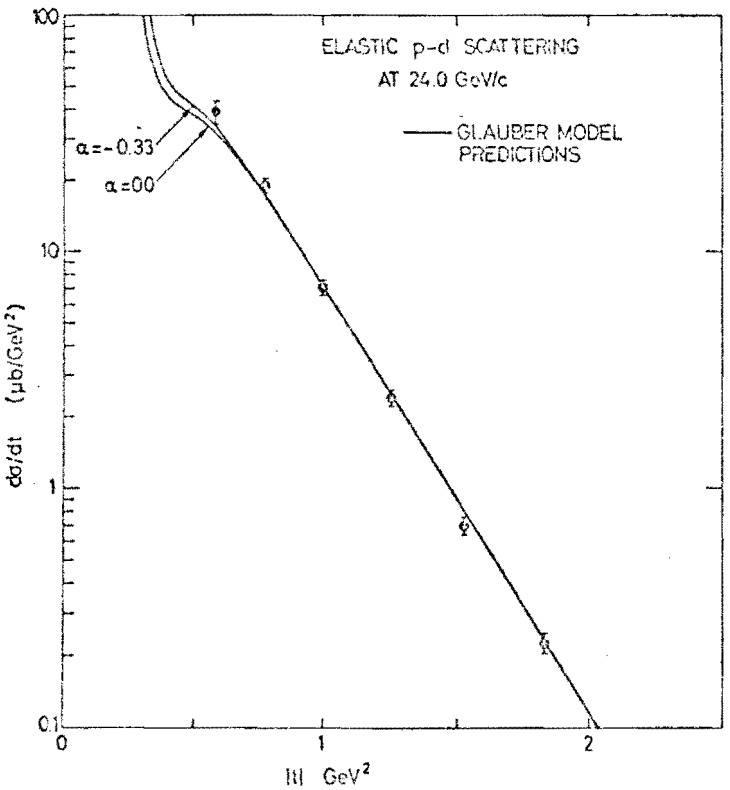

The results of elastic p – d scattering at 24.0 GeV/*c* are shown versus four-momentum transfer squared, $|t|$. The curves are Glauber-model calculations of elastic p – d scattering for two values of the ratio α of the real to the imaginary part of the p – p and p – n scattering amplitude.

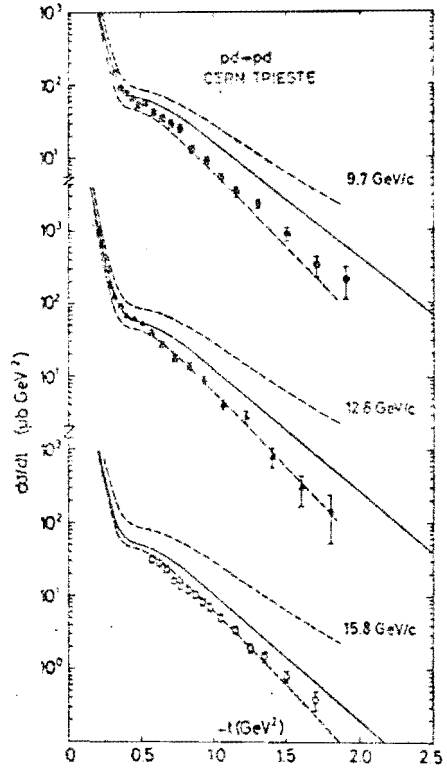

The pd elastic differential cross-section at 9.7 (●), 12.8 (▲), and 15.8 (■) GeV/*c*.

Fig. 4 p-d Elastic Scattering

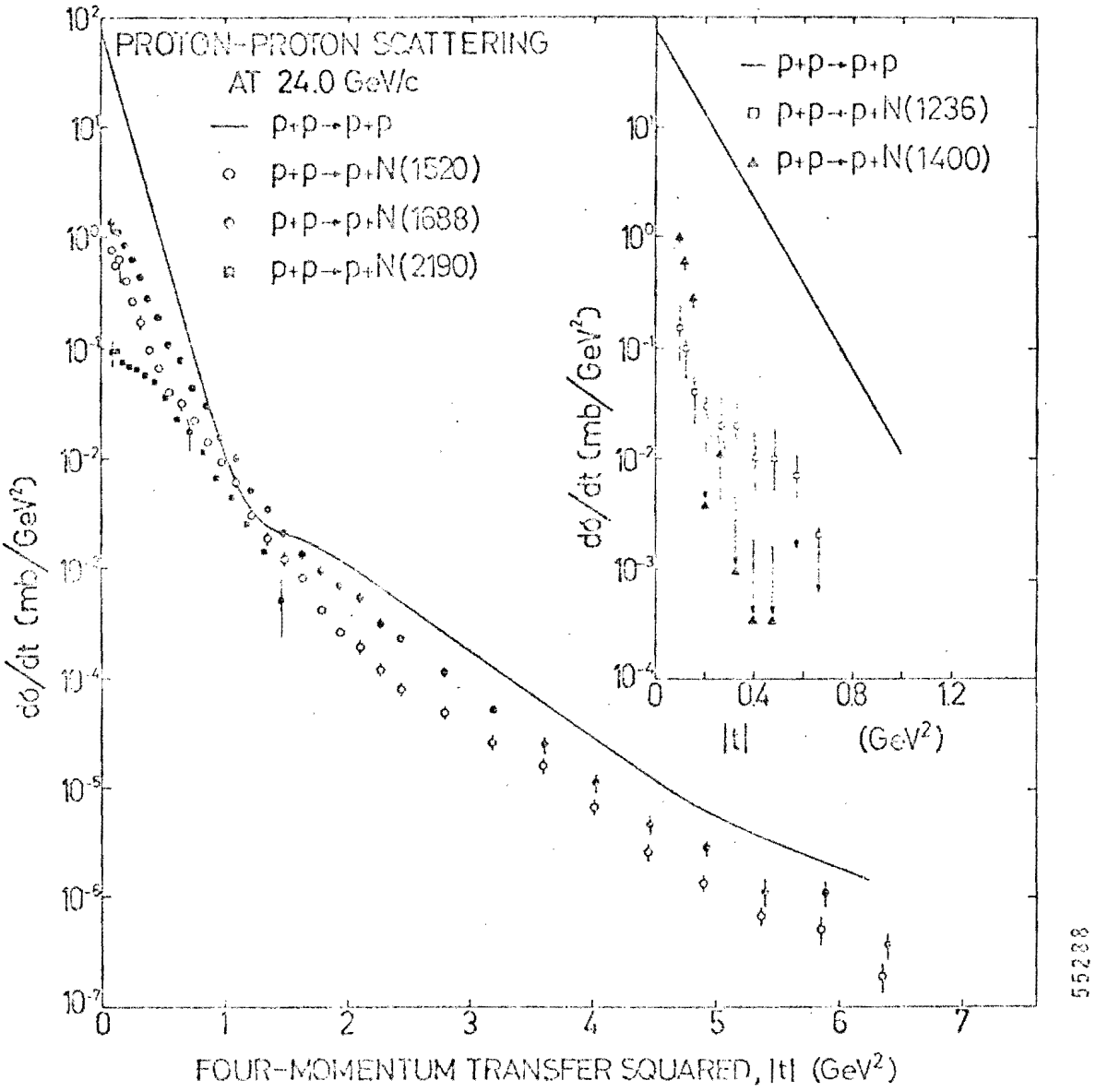

Fig. 5 Isobar Production at 24 GeV/c

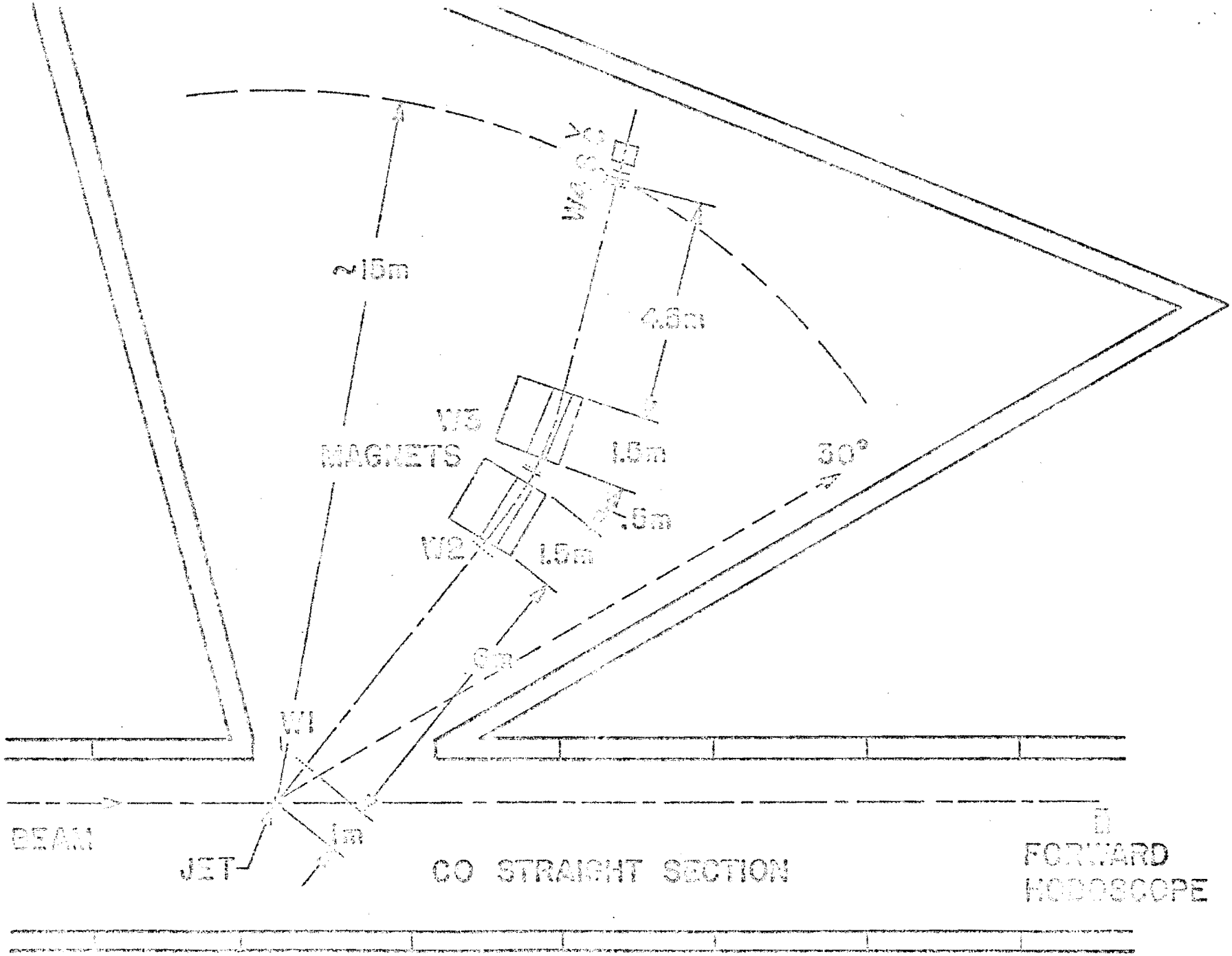

Fig. 6A Plan View of Experimental Setup

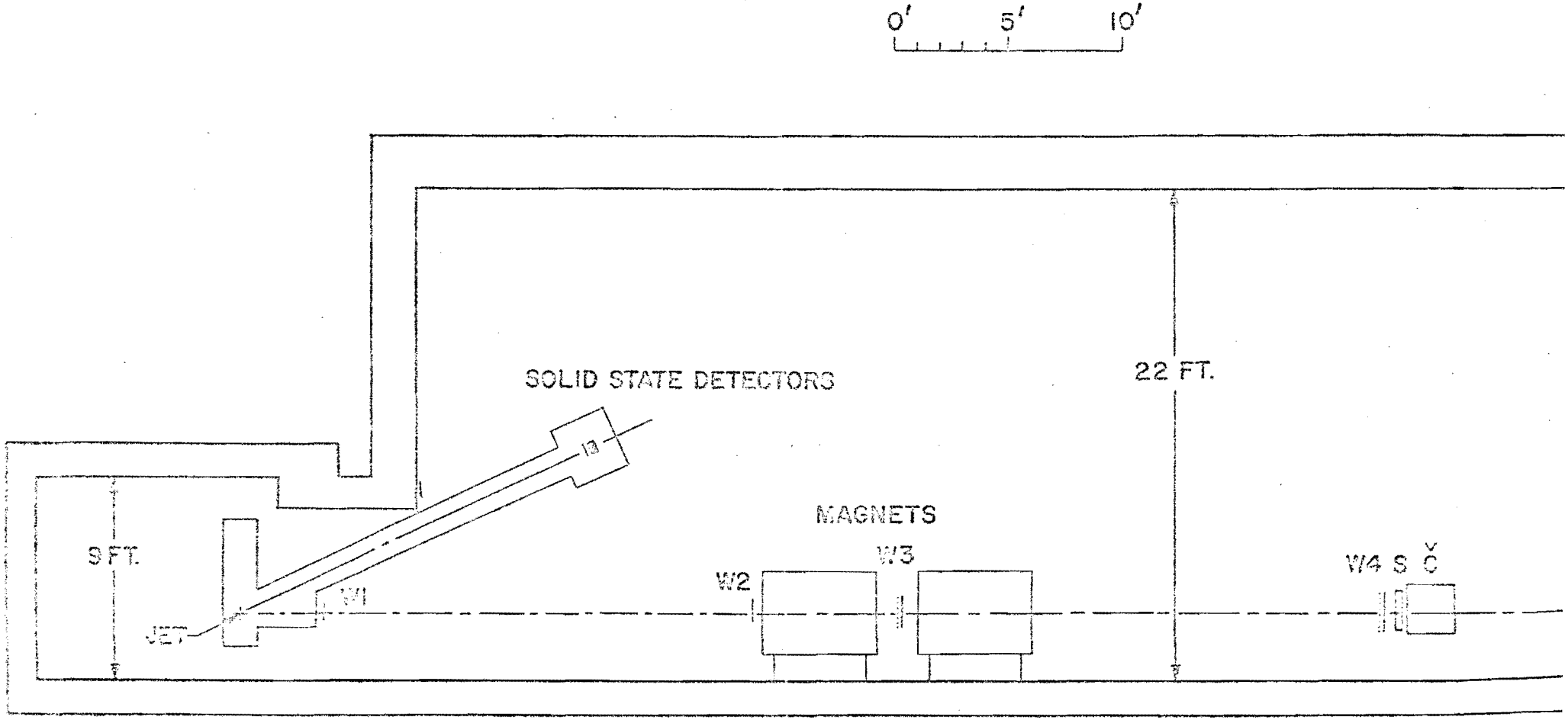

Fig. 6B. Elevation View of Experimental Setup

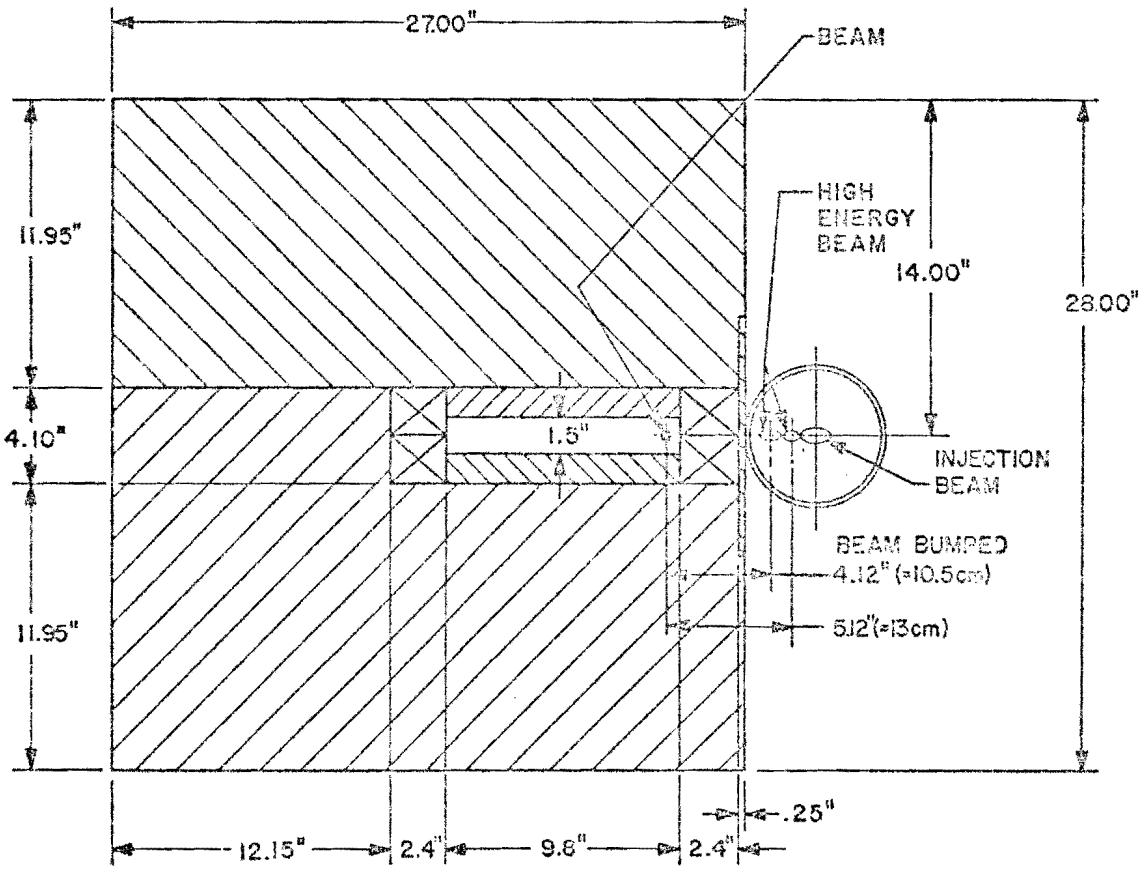

FIG. 7B CROSS SECTION of FORWARD MAGNET

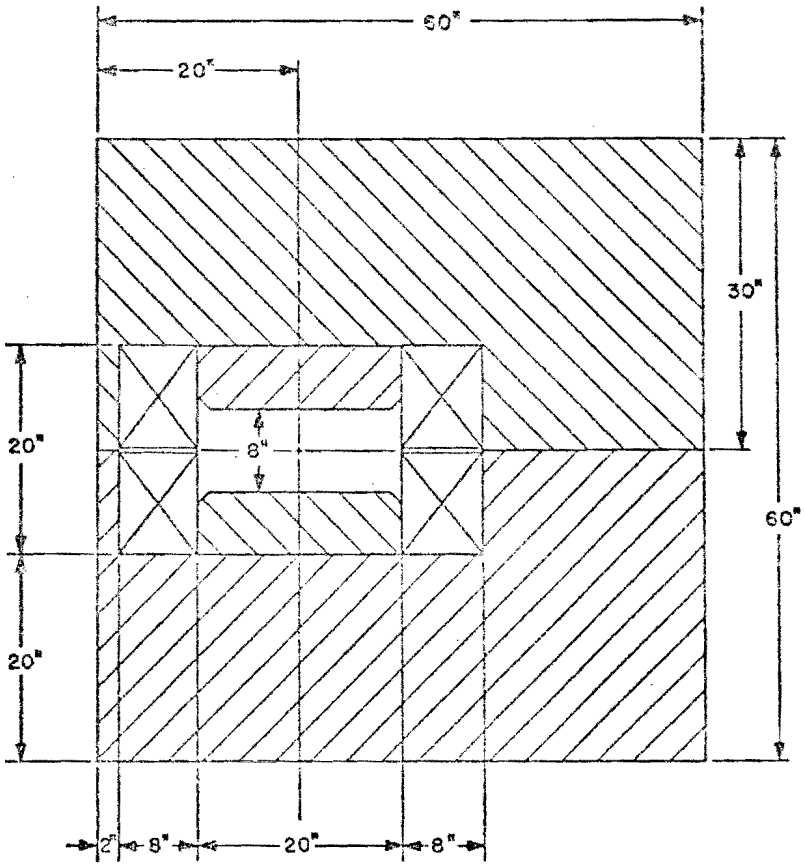

FIG. 7A CROSS SECTION of RECOIL MAGNET

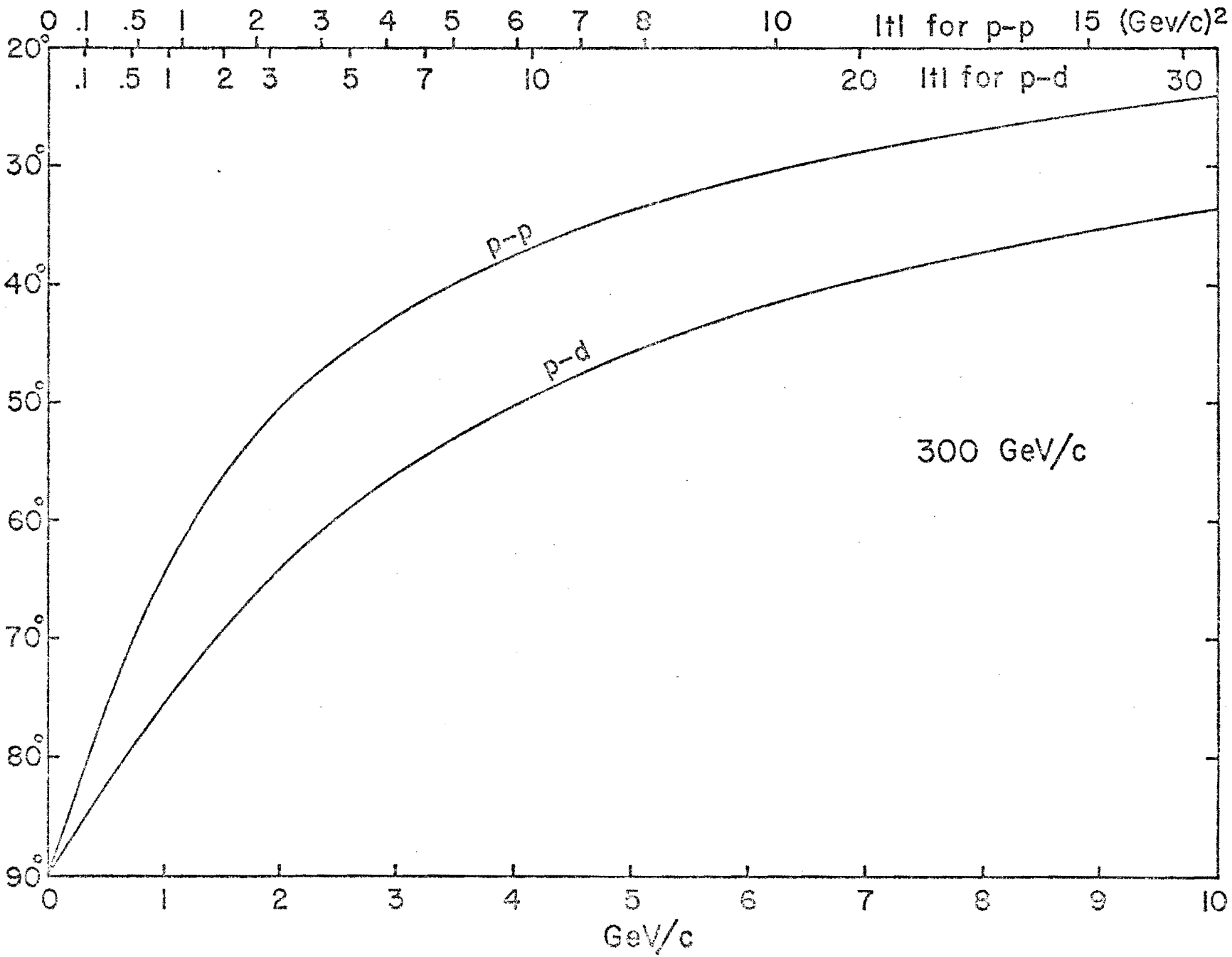

FIG 8 KINEMATICS OF RECOIL PARTICLES

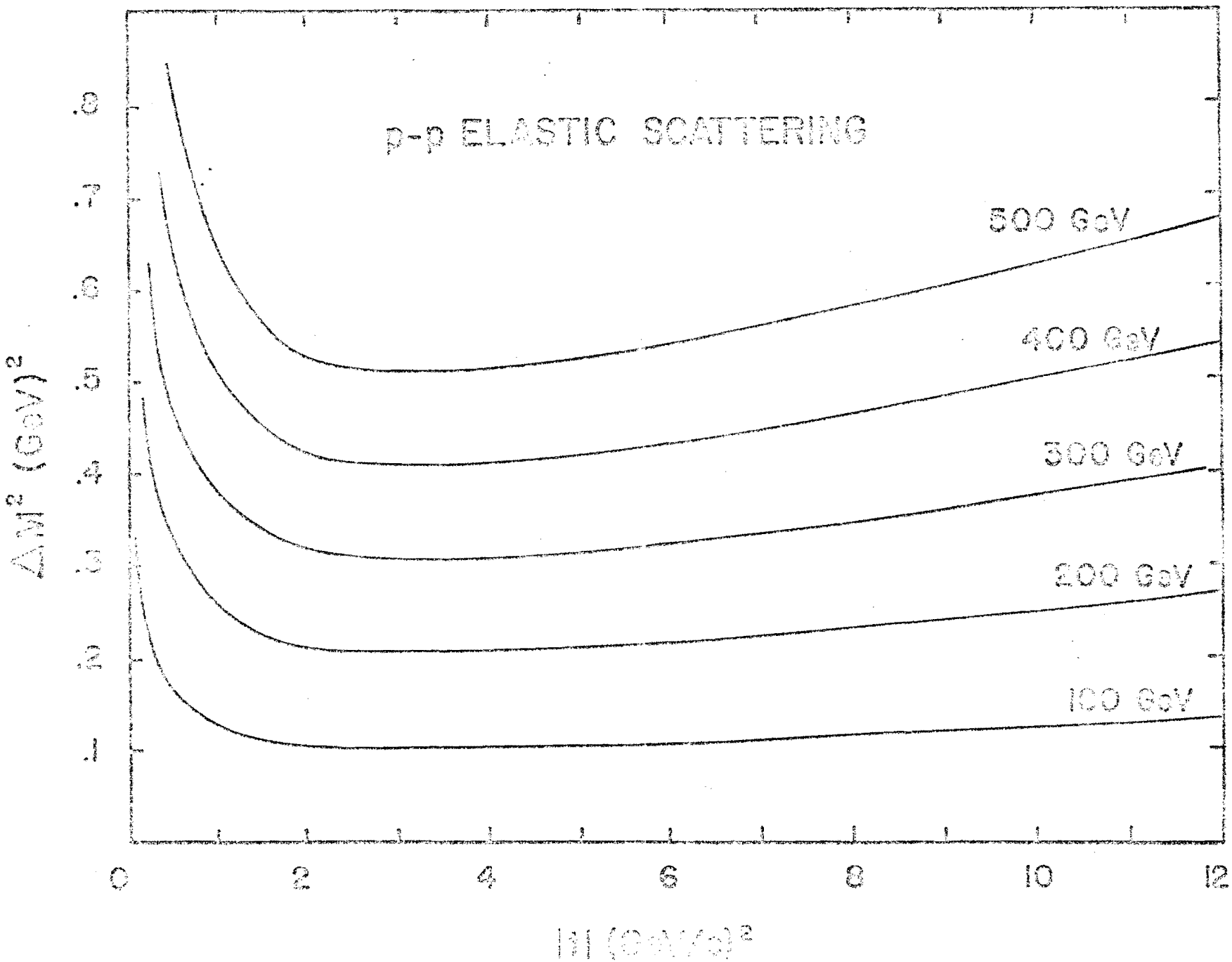

Fig. 9A. Missing Mass Squared Resolution as a Function of $|t|$ for Proton-Proton Elastic Scattering.

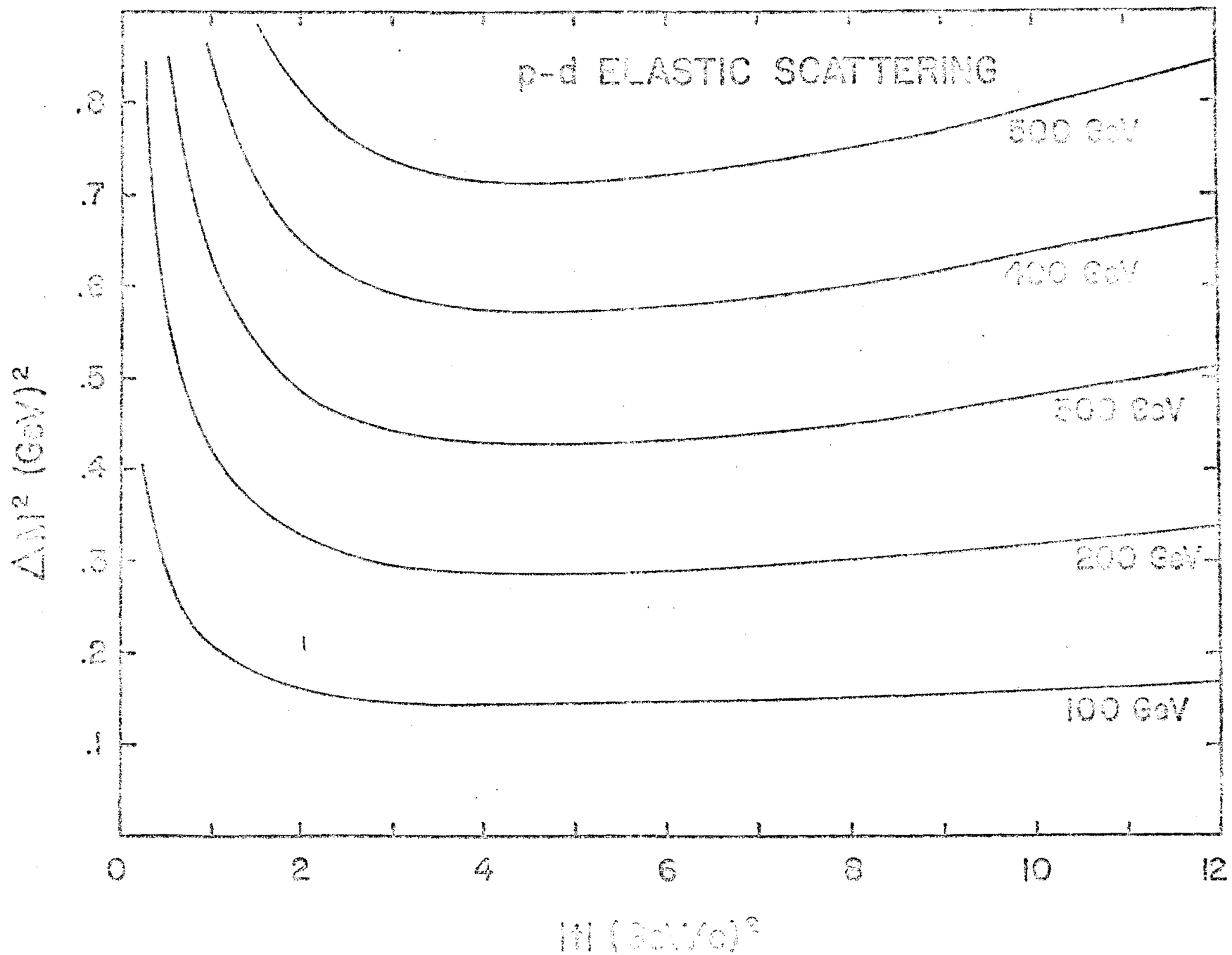

Fig. 9B. Missing Mass Squared Resolution as a Function of |t| for Proton-Deuteron Elastic Scattering.

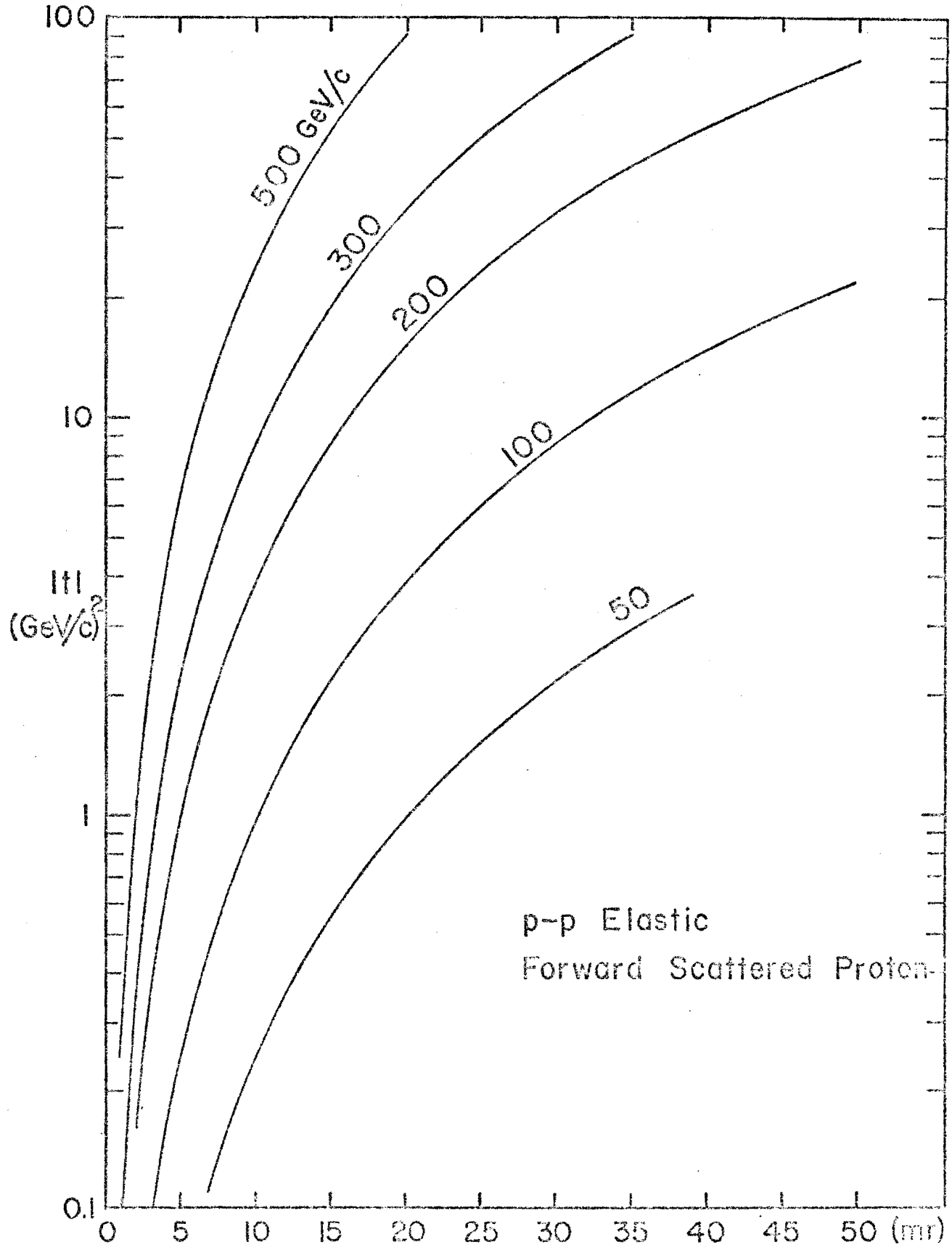

FIG. 10 KINEMATICS OF FORWARD SCATTERED PROTON

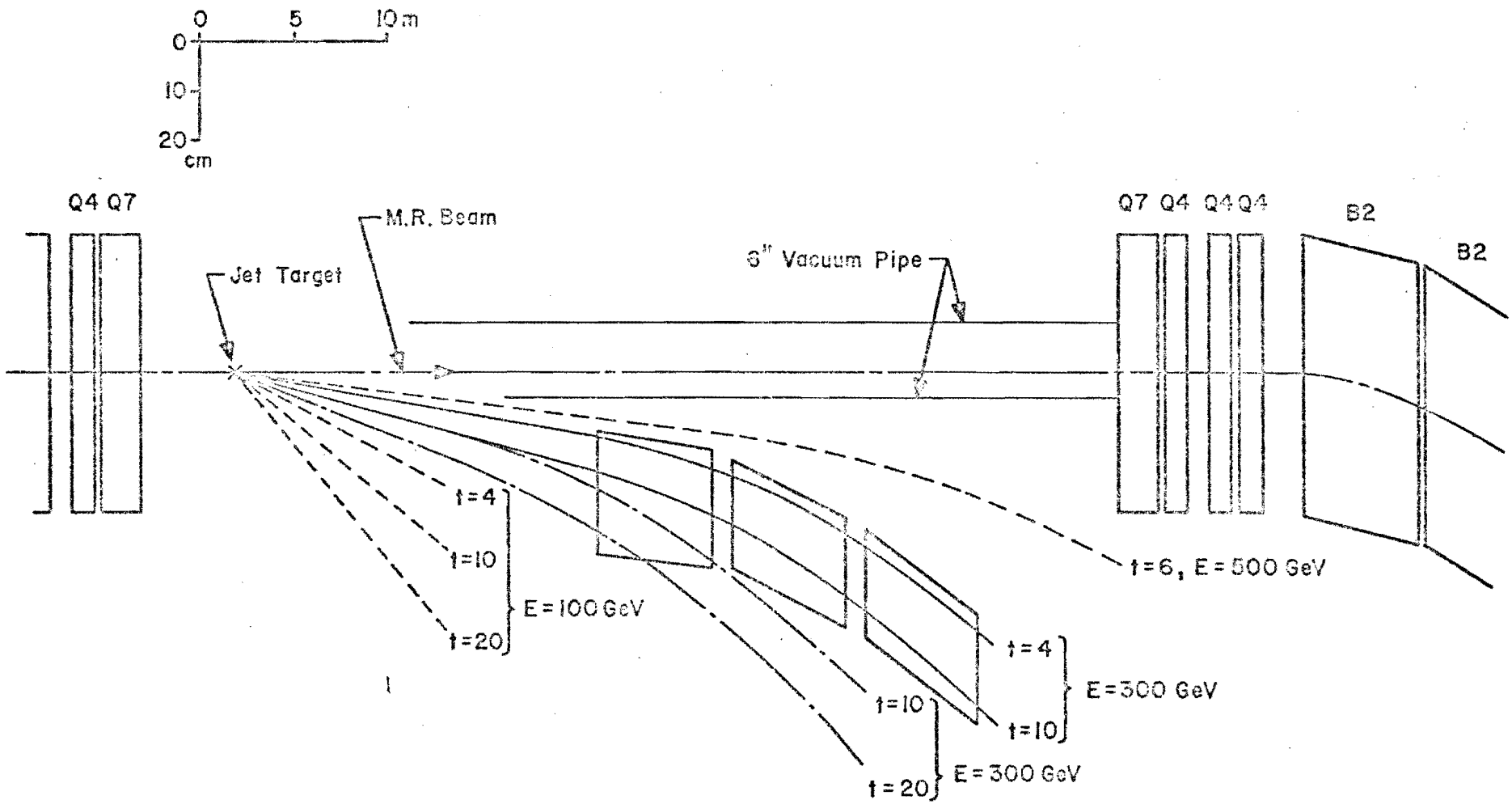

Fig.11 Position of Forward Spectrometer

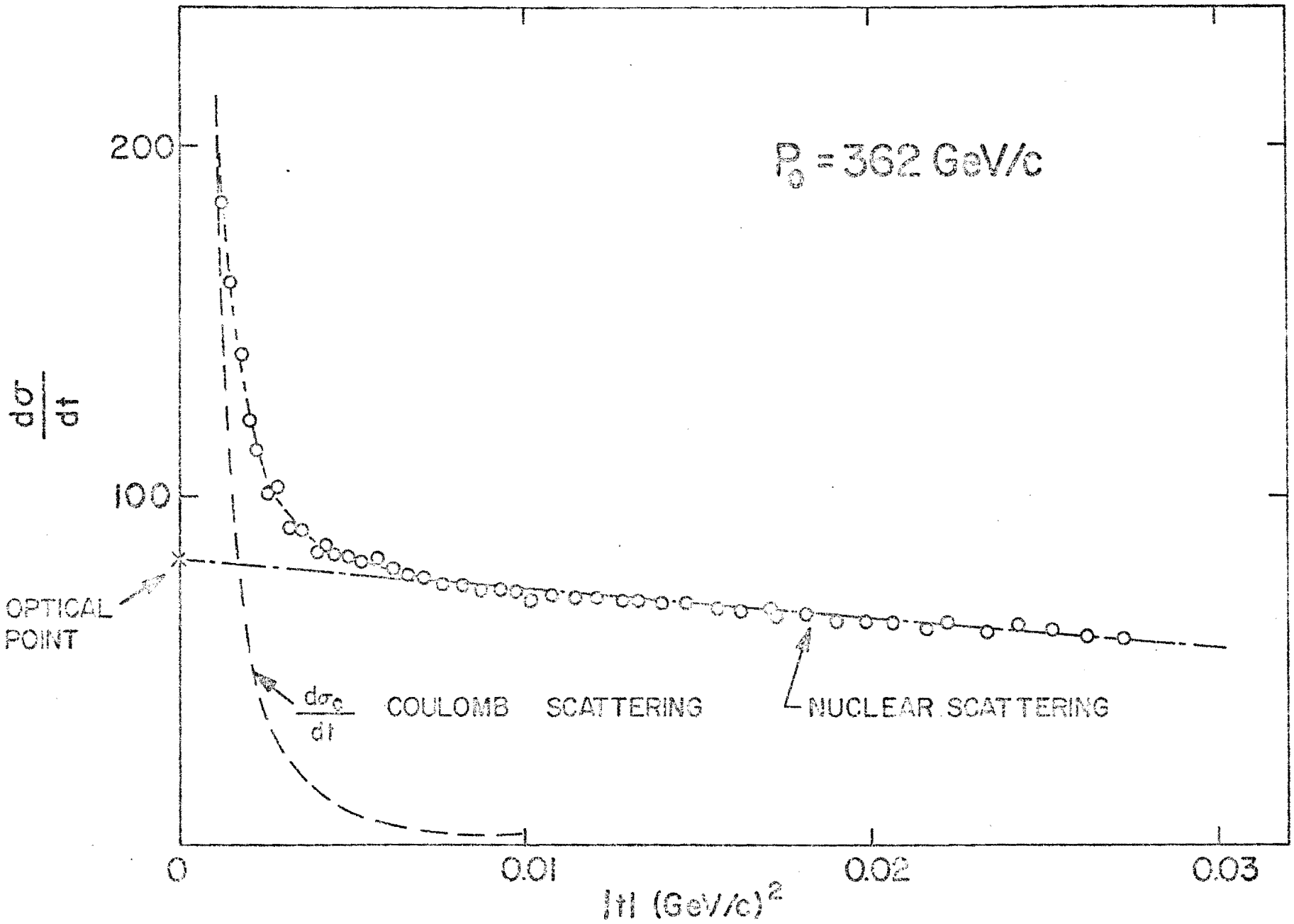

FIG. 12 DIFFERENTIAL CROSS SECTION

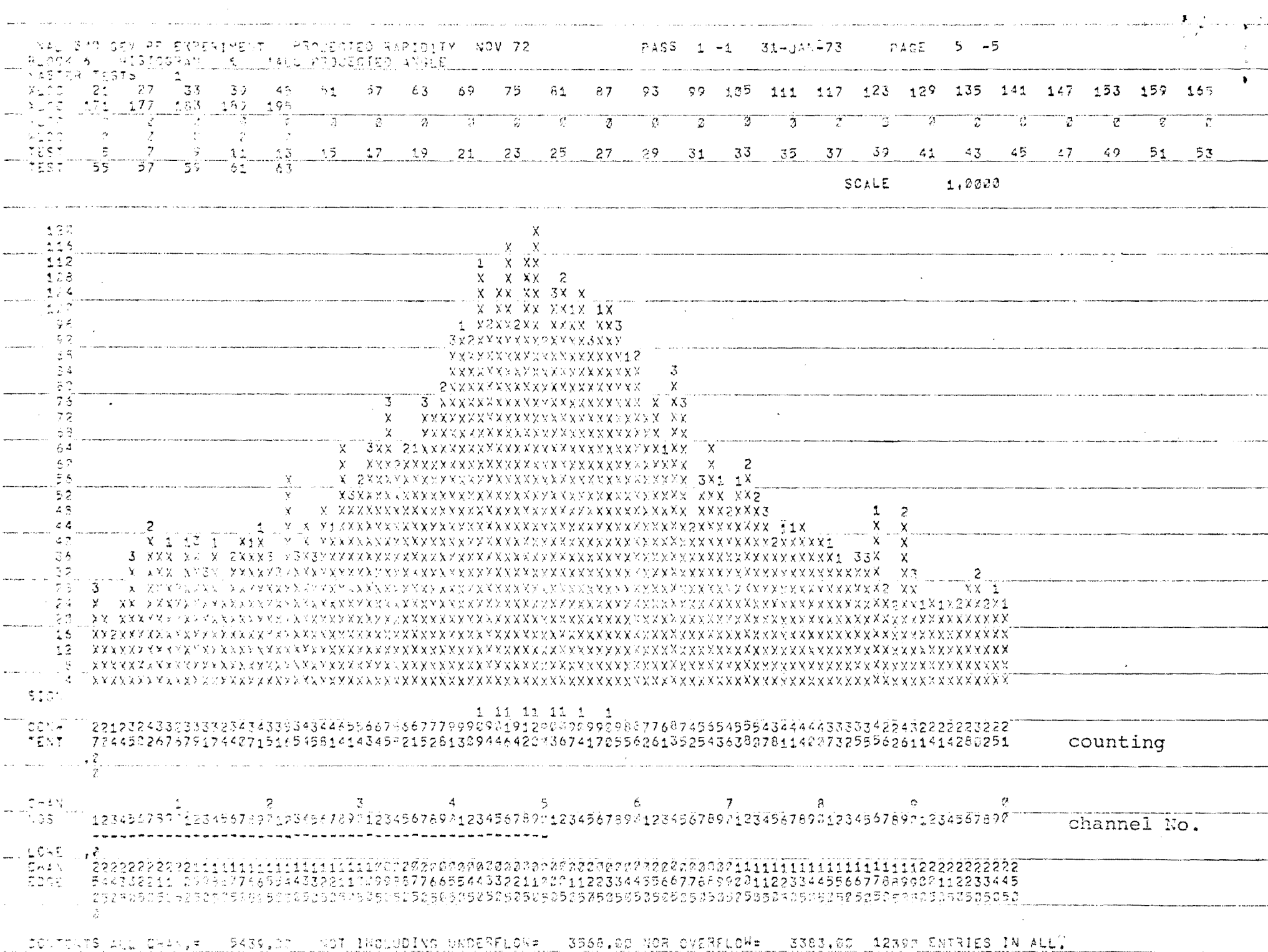

Fig. 13 Projected Angular Distribution of p-p reaction at 303 GeV/c in units of 5 mr

Correspondent: R. Yamada
NAL
Batavia, Ill.
Tel.: 312-840-3795

p-p and p-d Elastic and Inelastic Scattering in the High t-Region in the New Internal Target Laboratory

V. Bartenev, A. Kuznetsov, B. Morozov,
V. Nikitin, Y. Pilipenko, and L. Zolin

Joint Institute for Nuclear Research (Dubna)

and

E. Malamud and R. Yamada

National Accelerator Laboratory

and

F. Loeffler, E. Shibata, K. Stanfield and Y. Tang

Purdue University

June 25, 1973

ABSTRACT

We propose an experiment to measure p-p and p-d elastic and inelastic scattering in the high t-region in the new B-0 Internal Target Laboratory. These measurements will continuously cover incident beam energies from 30 to 500 GeV. We will cover the t-region from 0.2 up to at least 10 $(GeV/c)^2$ for p-p elastic scattering and up to 5 $(GeV/c)^2$ for p-d elastic scattering; we can go higher with future modifications. Magnetic spectrometers will be used to measure the angles and momenta of the recoil particle and the forward scattered particle.

1. Introduction

Small angle p-p elastic scattering up to 0.2 $(GeV/c)^2$ has been measured at the C-0 straight section by Experiment 36. The slope parameter and the real part of the scattering amplitude for p-p elastic scattering and the total cross section were measured.[1] Some of the same parameters for p-d elastic scattering were also measured[2] and will be measured in much more detail in the near future by Experiment 186.

In these measurements solid state detectors are used to define the scattering angle and the energy of the recoil particles for determination of elastic events. These measurements are limited to the very small t-range due to thickness of the solid state detector which defines the maximum detectable energy of the recoil particles.

We propose to measure elastic scattering from where the above experiment stops, up to about 10 $(GeV/c)^2$, and possibly into higher t-regions. The energy range covered will be from about 30 GeV up to 500 GeV. In the internal target area we have the added advantage that all incident energies are readily available up to the maximum machine energy. The s-dependence of the reactions can be determined easily. At low-t where only the recoil particle is measured, different energy data will be taken within the same main ring cycle. At high-t, where both recoil and forward scattered protons are measured, data will be taken by moving the magnets remotely within a short time.

Most of the equipment which we propose can be used for many future experiments, including these same experiments extended to 1000 GeV with the proposed energy doubler. Likewise, when the new internal target area

is built, it will be used by many other experiments, and will be the first experimental area for the beam from the energy doubler.

2. Physics

Elastic scattering may be divided into regions according to the t-range covered as shown in Table 1 for p-p elastic scattering and Table 2 for p-d elastic scattering. The data are divided according to their phenomenological behavior. Regions 1 and 2, for p-p and p-d, will be measured in Experiment 36 and 186. We will extend these measurements in the new internal target laboratory to higher t and higher s-regions.

2.1 p-p Scattering

Elastic p-p scattering at very high energy and at high-t up to 5 $(GeV/c)^2$ has been measured at the ISR and reported[3] as shown in Fig. 1. There is extensive data below 30 GeV, but there is not enough data between 30 GeV and ISR energies. We can measure elastic scattering in the NAL energy range and thereby provide this fundamental data in the gap between 30 GeV and ISR energies.

The most prominent feature of the ISR data may be the dip around 1.3 $(GeV/c)^2$ as shown in Fig. 1. This had not been observed at lower energies, although a kink in the cross sections exists there. This dip was predicted by many models for the asymptotic limit.[4] According to theory, this dip is partially filled in at low energy where the real part of the scattering amplitude is large. Preliminary data from Experiment 36 finds the ratio of the real to the imaginary part of the scattering amplitude to be less than 10% around 200 GeV and up (Fig. 2). Therefore,

we should be able to observe this dip and its s-dependence at NAL energies. Its relation to the real part of the scattering amplitude will be studied.

The theory also predicts another dip around $|t| = 5 \sim 8$ $(GeV/c)^2$. If this dip exists, our counting rate is high enough to find it. The internal target has an advantage over the ISR as far as counting rate is concerned. As is described in a memo by E. Malamud,[5] the interaction rate per second for $\sigma = 40$ mb is 10^4 for the ISR with a 10 ampere current, while that of a jet target is 7×10^8 with a proton density of 5×10^{-7} g/cm^2 and a beam intensity of 10^{13} ppp. Thus, our rate is about 10^5 higher than that of the ISR. We will have better statistics and will be able to measure into the higher t-region where the cross section is smaller. The data of Fig. 1 ends around $|t| = 5$ $(GeV/c)^2$, and we will be able to extend these results to $|t| \approx 10$ $(GeV/c)^2$. With future improvements in the jet target it may be possible to go to even higher momentum transfers.

2.2 p-d Scattering

The differential cross section for p-d elastic scattering was measured up to 2 $(GeV/c)^2$ at CERN using the PS up to 24 GeV/c.[6] This result is shown in Fig. 3. The dip around $|t| = 0.3$ has been investigated at lower energies extensively in other laboratories. Recently, Glauber has suggested that it may be due to the strong dependence on polarization of the deuteron spin and the d-state admixture[7]. Beyond 2 $(GeV/c)^2$ no data exists even at low energy. Only the NAL machine has the capability to investigate this region.

From the p-d elastic scattering we can also deduce information about p-n scattering.[8]

2.3 Isobar Production

In the previously mentioned measurements of p-p and p-d elastic scattering, we will measure the momentum spectrum of the recoil protons. With sufficient resolution we can measure the cross sections for isobar production.

The production of isobars having masses of 1236, 1400, 1520, 1688, and 2190 MeV in p-p reactions has been investigated quite extensively up to $|t| = 6$ $(GeV/c)^2$ and $P = 24$ GeV/c.[9] These results show that the differential cross sections for the 1520, 1688, and 2190 isobars have relatively small slope parameters ($b = 3 \sim 5$) and that they are comparable to that for elastic scattering around $|t| = 1$ $(GeV/c)^2$ as shown in Fig. 4. Moreover, the cross sections for producing these isobars are roughly s-independent up to 24 GeV/c.

As shown in Fig. 9, our mass resolution on the recoil particle using only the recoil arm is good enough to separate the isobars at 100 GeV beam energy for $0.2 \lesssim |t| \lesssim 6$ $(GeV/c)^2$. At higher beam energies the separation of isobars becomes more difficult, especially between the 1520 and 1688 isobars. Thus, we expect to measure isobar production cross sections certainly at 100 GeV and perhaps up to 300 GeV in incident energy.

3. Experimental Setup

The proposed experimental setup is shown in Fig. 5. A magnetic spectrometer is used to define the angle and momentum of the recoil particle and a

forward spectrometer is similarly employed for forward scattered particles. A set of monitors will also be provided in the tunnel.

For the low $|t|$ region as shown in Fig. 9, only the recoil spectrometer need be used. Its resolution is sufficient to define elastic events, especially at lower energies. For the higher $|t|$ region, both spectrometers are used. Scintillation counter hodoscopes are used in the forward spectrometer; the angle information and the momentum of the forward particle are used together with the information from the recoil spectrometer to define the coplanarity and elasticity of the event. Four parameters are measured and the elasticity of the event is therefore over-defined (the momentum and the angle of a recoil particle, and of a forward scattered particle are measured).

3.1 Recoil Particle Spectrometer

At large fixed angles momentum and t-value of elastic recoil particles change very little when the incident beam energy increases. The angle and the momentum of the recoil particle is shown in Fig. 6 for 300 GeV/c incident momentum. As was suggested in a note by R. Carrigan,[10] it is reasonable to use a magnetic spectrometer where high t-values are studied. We propose to make a magnetic spectrometer with two bending magnets and a proportional chamber system for recoil particles in the B-O section as shown in Fig. 7. We will be able to use this spectrometer up to $|t| = 15$ $(GeV/c)^2$ in steps of 5 degrees.

The spectrometer consists of two magnets, four vertical and two horizontal proportional chamber planes and trigger counters. The relative position of these components to the target and beam line is

shown in Fig. 7. The whole system is mounted on a carriage and will be remotely rotated around the center of the target. The carriage supports two magnets, proportional chambers, trigger counters and some electronic circuits. There will be some provision to change the relative angle of the two magnets on the carriage for different deflection angles.

The first two wire planes define the incident angle of the recoil particle using only vertical wires. They will be placed about 0.5 and 2.5 meters from the target. The vertical wires will have 1 mm spacing. The polar angle will be defined with an accuracy of $\sim \pm .4$ mrad. The recoil particle line will be extrapolated back to the target to check that it originated in the target.

There is a set of vertical and horizontal chambers between the two magnets, and another similar set two meters downstream from the second magnet. These also have one millimeter wire spacing vertically and two millimeters spacing horizontally. The 6.3 and 2.9 GeV/c protons, corresponding to $|t| = 10$ and 4 $(GeV/c)^2$, will be bent by 14.7 and 32.1° at 18 kG respectively. The momentum resolution ($\Delta p/p$) will be about .15 and .08% respectively.

The solid angle is defined by the scintillation counter S1, which subtends about 2.2 msr in the lab system and covers five degrees in the polar angle. The aperture at the entrance of the first bending magnet must be 21.9 cm wide and 6.3 cm high to cover the solid angle. The apertures of the bending magnets are larger than these dimensions (5 inches high and 20 inches wide). The magnets bend the recoil particle in horizontal plane as indicated in Fig. 7. The proposed shape of the magnet is shown in Fig. 8A. It is almost a C-shaped magnet having only

a thin yoke on the beam side which acts as a magnetic shield for the main ring and gives structural strength. Although we are describing conventional magnets, we should like to use super-conducting magnets whenever they become feasible.

The solid angle defining counter S1 is at the end of the spectrometer as is a second scintillation counter, S2. An absorber and a Cherenkov counter are placed between them. A signal derived from the coincidence of S1 and S2 will be used to register events into the computer. In addition, a coincidence is required with the RF structure of the main ring beam to avoid events not originating in the target. Pulse height in the Cherenkov counter will be recorded and used to help eliminate background due to pions.

Time of flight will be used at low t-values only. The time of flight difference between a 2.9 GeV/c pion and a proton of the same momentum ($|t| = 4$ $(GeV/c)^2$) is about 1 ns.

3.2 Mass Resolutions

Measuring only the recoil proton, the missing mass squared of the forward scattered particle is given by

$$M^2 = m_o^2 + 2m_r^2 + 2m_r\,(E_o - E_r) - 2\,(E_o E_r - p_o p_r \cos\theta_r).$$

Here the subscripts o and r refer to the incident and recoil particles respectively. Thus, the missing mass resolution can be estimated by taking

$$\Delta M^2 = \left[\left(\frac{\partial M^2}{\partial p_o}\right)^2 (\Delta p_o)^2 + \left(\frac{\partial M^2}{\partial p_r}\right)^2 (\Delta p_r)^2 + \left(\frac{\partial M^2}{\partial \theta_r}\right)^2 (\Delta \theta_r)^2\right]^{\frac{1}{2}}.$$

The results of our calculations are shown in Fig. 9. We have taken into account multiple scattering in the vacuum chamber windows and proportional chambers and also the position measurement error in the chambers.

If we insist on having resolution better than the separation between the elastics and the $N^*(1520)$, say $\Delta M^2 \approx .7$ (GeV/c)^2 or $\Delta M \approx 370$ MeV then, as may be observed in Fig. 9, we can measure from $|t| = .2$ to $|t| = 10$ (GeV/c)^2 at 100 GeV/c. At 300 GeV/c we can measure from $|t| = .3$ up to $|t| \approx 9.0$ (GeV/c)^2 with only the recoil spectrometer. At the higher energies and momentum transfer values both spectrometers are required to separate elastics from the N^*'s. For example, at 300 and 400 GeV/c the forward spectrometer acceptance begins at $|t| = 1.0$ and $|t| = 1.8$ (GeV/c)^2 respectively. Thus, for energies below 300 GeV we will measure the angular distribution starting at $|t| = .2$ and continue on up to about $|t| = 10$ (GeV/c)^2. At energies above 300 GeV our measurements will begin at some lower cut-off (e.g., $|t| = 1.8$ (GeV/c)^2 at 400 GeV) and continue to the higher t-values.

3.3 Forward Particle Spectrometer

As is shown in Fig. 10, the forward scattered particles at fixed angle have increasing momentum and t-values as the circulating beam energy increases. Therefore, the system at a fixed position with a fixed current measures elastic scattering for one energy only. The laboratory angle for the forward scattered particle at $|t| = 4$ (GeV/c)^2 is 6.9, 5.2, and 4 mr for 300, 400, and 500 GeV beams respectively.

The system consists of three bending magnets and four sets of scintillation counter hodoscopes as indicated in Fig. 6. At 300 GeV the front end of the first magnet is placed 19.1 meters downstream from the jet target in order to cover the t-region from 4 to 10 $(GeV/c)^2$. The current in the magnets as well as the position and angles of the magnets will be adjusted to accept only the elastically scattered protons. The momentum acceptance, which should be about 0.5%, can be easily achieved and the necessary horizontal acceptance is 2 mr. The solid angle is defined by the recoil spectrometer.

The scintillation counter hodoscopes are before the first magnet, between magnets, and after the last magnet in the forward spectrometer. There are also some anticoincidence counters to veto particles scattered from the steel surface and from the outside. Each hodoscope consists of twelve horizontal and six vertical scintillation counters. With the information from the forward spectrometer the coplanarity and elasticity of the events will be determined, and we can select the elastically scattered protons from the background. If necessary, proportional chambers will be installed near the end of the forward spectrometer to improve resolution. For completeness we show the layout of the forward spectrometer for a different energy in Fig. 11.

The magnets are similar to the main ring magnets as far as aperture and length are concerned. The steel core is shaped like the recoil spectrometer, as shown in Fig. 8B. The outside dimensions will be about 28 inches high and 27 inches wide.

The first magnet has an aperture 1.5 inches high and 9.75 inches wide with a 16 turn coil. The inside yoke is 1/4 inch thick and the coil is 2.39 inches wide. Therefore, the particle can go through the magnet at a minimum distance of 2.64 inches from the outside surface. The second and third magnets have an aperture 2.0 inches high and 8.73 inches wide and 24 turn coils.

These magnets are connected in series and are excited by the same power supply to a magnetic field of about 18 kG with 3500 Amp. The resistance of the first and second magnets will be about 17 and 26 m Ω. The maximum total power consumption for these three magnets will be about 850 kW.

The main ring vacuum pipe at B0 will be shifted inward by one inch relative to the center line connecting the upstream and downstream quadrupole magnets. The injected beam will be centered in this pipe with local low field correction magnets. However, the high energy beam will be set to run 2 inches from the outer surface of the 6 inch pipe as shown in Fig. 9B. As the extraction septum in A0 is set at 3 cm outside the center line and the abort target in D0 is set at 1.5 inches, this would not seem to be a problem.

The use of a local magnetic field beam bump at high energy will be considered. With this modification the beam will be shifted outward to make a lower t-region accessible in the coincidence experiment.

3.3 Monitor

We will install a vacuum guide at right angles to the main ring beam line, which is about 4 meters long and covers laboratory angles

roughly from 90 to 80 degrees. At the end of it will be installed several fixed solid state detectors which will be used to monitor small angle elastic events as was done in Experiment 36. These will be used as a relative luminosity monitor.

We will also develop and install an absolute luminosity monitor, utilizing either light emission due to the beam hydrogen gas interaction or Coulomb scattering.

4. Counting Rates

The density of the hydrogen jet is about 5×10^{-7} g/cm^3. As the present beam interaction region is about 1 cm^3, we can assume $N_t = 3\times10^{17}$ proton/cm^2 is available as our target. The jet duration time is about 200 ms, and 3 or 4 jet pulses in a main ring cycle are now possible. Also, the jet may be pulsed for one second continuously. We will operate the jet during the ramp for lower t-values. For higher t-values we may use the flat-top or front porches of the main ring ramp.

The presently available beam intensity in the main ring is about 4×10^{12} proton/pulse; this will be increased eventually to 5×10^{13} proton/pulse. For these calculations we assume 1×10^{13} proton/pulse which may be a conservative value in the latter part of 1973. During a jet duration of 200 ms, the main ring beam circulates 10^4 turns around the ring. So effectively, the available beam during a jet pulse is $N_b = 10^4 \times 10^{13} = 10^{17}$ proton/pulse. We will operate one jet at low energy and another at higher energy where the forward spectrometer is adjusted. We will operate 2 or 3 jets during flat-top when it is feasible.

The counting rate, N, per jet pulse is given by the following equation:

$$N = N_b N_t \frac{d\sigma}{dt} \Delta t \frac{\Delta\varphi}{2\pi} = 3\times10^{34} \frac{d\sigma}{dt} \Delta t \frac{\Delta\Phi}{2\pi} \text{ / jet pulse}$$

N is given in Table 3, with the estimated $d\sigma/dt$ values from the presently available data. $\Delta\Phi$ is given by 6.3 cm/(250 cm x sin θ). The counting rate is defined by the solid angle of the recoil particle spectrometer since the forward particle hodoscope is made large enough to accommodate all the corresponding elastic events.

The Russian members of our collaboration are presently exploring the possibility of increasing the density of the jet for use at the highest t-values. One possibility is to reduce the velocity of the jet and another is to develop a solid hydrogen target. With such modifications the jet density may be increased by a factor of 10 or more. On the other hand the beam intensity may be raised to 5×10^{13} proton/pulse. With both these modifications the counting rate may be increased by a factor of 50 in the near future. Thus, the highest accessible t-value may be higher than discussed in this proposal.

5. Background Rate

There are two types of background: one target associated and the other not. The background which does not come from the target was measured in May 1973 at 300 GeV to be about 16 minimum ionizing particles/cm^2/sec/10^{10} circulating protons at 3.5 feet from the beam line.[11] Thus, at 13 cm from the beam line and with 10^{13} circulating protons, the corresponding number is 10^6 particles/cm^2/sec. Although this rate is tolerable for the forward hodoscope, it will be reduced by at least an order of magnitude. First of

all, the experimental area at B-0 will be designed more carefully so as not to restrict the circulating beam. Secondly a beam scraper at A17 and beam collimators at D-0 will be used.

The effect of the accidental rate due to particles coming from the target can be estimated for the forward spectrometer including the first forward hodoscope as follows. This hodoscope is more seriously affected than the recoil spectrometer. We estimate the background rate at the $|t| = 4$ (GeV/c)^2 setting at 300 GeV. As there is a maximum of 1113 beam bunches in the main ring, we have $N_b = 10^{10}$ proton/bunch for a beam intensity of 10^{13} ppp. The interval between beam bunches is about 20 ns and the total number of reactions during a bunch is estimated from a total cross section of 40 mb as follows:

$$N_b \; N_t \; \sigma_{tot} = 10^{10} \times 3 \times 10^{17} \times 40 \times 10^{-27} = 120$$

The multiplicity measured by the bubble chamber is about 8.9 at 303 GeV, and the projected distribution in one dimension is shown in Fig. 12, where the events are grouped in 0.5 mr bins.[12] Therefore, we have about 1000 charged particles coming from a jet target associated with a single beam bunch. The maximum number of particles going through the aperture of the first useful magnet opening (which is 4 mr horizontally and 1.5 inches high) is estimated to be less than 0.6%. Thus, on the average, 6 particles may go through this opening; we can easily select the elastic scattered proton from the information given by the following counter hodoscopes. As these 1000 charged particles may produce many low energy daughter particles when they finally hit vacuum chambers and magnets, it is preferable to use a thin vacuum tube and also to place the counter hodoscope so that the back

scattered particles reach the hodoscope out of phase with the scattered particles of interest, e.g., 10 ns later. The number of muons was measured in the CO area by Experiment 120.[13] They observed 500 μ/jet (=200 ms) /10^{12} proton at 250 GeV with a counter of 2/3" x 2/3" placed at 16 mr and at 32 feet downstream from the jet. This gives 2.5×10^{-3}/bunch (=20 ns) /10^{13} proton/2 msr at 16 mr. This number will not cause difficulty for this experiment.

6. Comparisons with Other Experiments

In the future, elastic scattering will be measured at NAL using the external beam. However, we can measure the elastic scattering of p-p and p-d in the main ring in a very flexible and efficient way. There are several advantages of the internal target experiment over external target experiments for these reactions:

A. It is possible to select the incident beam energy freely from the injection energy to the highest extraction energy. Thus the s-dependence measurement can be done easily and in a bias free way.

B. The internal target has the first access to the highest machine energy (500 GeV/c or even 1000 GeV/c because no slow extraction is involved).

C. The target is thin, so that the multiple scattering of the recoil particle is small compared to that of a liquid hydrogen target. Therefore, elastic scattering may be measured using only the recoil spectrometer over a large range of t (Fig. 9).

D. The luminosity for the internal target is comparable to that of the external beam. For the internal target with 3 pulses of 200 ms width and a beam intensity of 10^{13} ppp, $L = N_b N_t = 10^{13} \times 3 \times 10^4 \times 5 \times 10^{-7} \times 6 \times 10^{23} = 0.9 \times 10^{35}$. For the external beam with 4×10^{11} ppp and 4" long liquid hydrogen target we have:

$$L = N_b N_t = 4 \times 10^{11} \times 4 \times 2.54 \times 0.071 \times 6 \times 10^{23} = 1.7 \times 10^{35}$$

E. At the internal target the incident beam has no pion contamination; identification of incident particles using Cherenkov counter is therefore not necessary.

7. Apparatus

We are assuming the construction of the B0 internal target area will be started sometime in 1973. Allowing six months for construction of this area, we expect the experimental area will be ready for occupation in early 1974. While the experimental area of the B0 straight section and the service building are under construction, we will work on preparations for the experiment.

The major items which should be made or purchased during that time are:

A. B0 general facility

1. Jet target
2. Control system for jet target
3. Helium liquifier, including dewars
4. Transfer line for helium
5. Recovery system of gases
6. Beam bumping, possibly using local bump magnets

7. Monitors (beam intensity, beam position, elastic monitor, etc.)

8. Communication system (TV, utility crate)

We assume NAL will supply all of these except for the jet target, which will be built by the Soviet collaborators. All of these are similar to the equipment presently in CO, and we expect all of it to be duplicated and completed in nine months.

B. Experimental equipment

1. Recoil spectrometer magnets

2. Forward spectrometer magnets

3. Power supplies for spectrometers

4. Cooling system for spectrometers

5. Fast logic circuits

6. Proportional chamber system including Camac and its interface

7. Scintillation counter hodoscopes

8. On-line PDP-11 system

We request NAL to supply the spectrometer magnets and power supplies as well as the cooling system. Purdue University will build the proportional chambers and all scintillation counters. NAL will supply the readout electronics for the chambers, the PDP-11, Camac and its interface.

8. Experimental Procedure

We will first study p-p and p-d elastic and inelastic scattering in the lower t-region up to 4 $(GeV/c)^2$ with continuous incident energies using only the recoil arm. For this phase of the experiment we need about 400 hours of running time.

Next, using both the forward and recoil spectrometers, we will measure p-p elastic scattering in the high t-region with 200, 300, 400 and possibly 500 GeV beams. This experiment needs about 600 hours of running.

Thus, we are requesting a total of 1,000 hours of running time for all experiments. Within one month after we move into the new service building, we will be able to start the experiments. Members of our collaboration started the CO Internal Target Area and also helped carry out other experiments. This has provided a driving force in CO and we expect to provide a similar driving force in the new BO Internal Target Area.

9. Possible Future Experiments

The elastic scattering experiment we propose to do should be the first experiment in the new Internal Target Area; it will provide data essential to understanding the apparatus for further experiments. Using the same equipment and with some modifications the apparatus can also do the following experiments.

9.1 $p+p \rightarrow p$ + anything

9.2 $p+p \rightarrow \pi^{\pm}$ + anything

These two reactions will be very interesting to study over the entire s-range. We can do these experiments by adding suitable Cherenkov counters to the recoil arm.

9.3 Elastic scattering from some nuclei

Elastic scattering from some nuclei can be measured using the same equipment by observing the recoil nuclei with the low momentum spectrometer.

9.4 Polarization measurement

A carbon polarizer can be placed after the first magnet of the recoil spectrometer in order to measure the left-right assymmetry with use of an extra set of wire chambers. A polarization measurement in the region around the dip at $|t| = 1.3$ $(GeV/c)^2$ should help provide an understanding of the mechanism responsible for the dip.

9.5 $p+p \rightarrow \pi^+ + d$

10. Manpower

In addition to the physicists listed on the title page, we expect one or more people from NAL and at least one graduate student from Purdue University to join the experiment when it is approved.

References

1. V. Bartenev et al., P.R.L. 29, (1972) 1755.
2. R. Yamada et al., A.P.S. New York meeting, 1973.
3. U. Amaldi, CERN NP Internal Report 73-5, April 1973.
4. L. Durand III, and R. Lipes, P.R.L. 20, (1968) 637.
   T. T. Chou and C. N. Yang, P.R.L. 20, (1968) 1213.
5. E. Malamud and W. Pelczarski, Proposal for a New Internal Target Hall.
6. F. Bradamante et al., Phys. Letters 32B, (1970) 303.
   U. Amaldi et al., Nuclear Physics B39, (1972) 39.
7. V. Franco and R. J. Glauber, P.R.L. 22, (1969) 370.
8. U. Amaldi et al., Nuclear Physics B39, (1972) 39.
   G. Bezongikh et al., "Determination of Deuteron Form Factor From Experimental Data on Elastic p-d, p-p and n-p Scattering at Small Angles in the Energy Range of 10-26 GeV". Dubna Preprint (1972).
9. J. V. Allaby et al., Nuclear Physics B52, (1973) 316.
10. R. Carrigan's note "Extension of Proton Scattering Internal Target Techniques to Larger Momentum Transfer" March 31, (1970).
11. J. Johnson. Private communication.
12. J. Schivell. Private communication.
13. R. Imlay. Private communication.

Table 1 - pp Elastic Scattering (at 300 GeV/c)

	t range	Recoil Proton P (GeV/c)	E (GeV)	Angle (°)	Scattered Proton P (GeV/c)	Angle (°)	Physics
1.	$0<t<0.01$	$P<0.1$	$E<0.005$	$\theta>87$	$=300$	<0.02	Coulomb Interference Real Part
2.	$0.01<t<0.2$	$P<0.46$	$E<0.11$	$\theta>76.5$	$=300$	<0.09	Break in b
3.	$0.2<t<1$	$P<1.2$	$E<0.55$	$\theta>61.5$	>299.5	<0.19	
4.	$1<t<10$	$P<6.2$	$E<5.4$	$\theta>42$	>294.6	<0.61	Dips
5.	$10<t<100$	$P<54.3$	$E<53.3$	$\theta>9.6$	>246.5	<2.1	
6.	$100<t$						

Table 2 - pd Elastic Scattering (at 300 GeV/c)

	t range	Recoil Deuteron P (GeV/c)	E (GeV)	Angle (°)	Scattered Proton P (GeV/c)	Angle (°)	Physics
1.	$0<t<0.01$	$P<0.1$	$E<0.003$	$\theta>88.5$	$=300$	<0.02	Coulomb Interference Real Part
2.	$0.01<t<0.2$	$P<0.45$	$E<0.053$	$\theta>83.2$	$=300$	<0.09	Single Scattering
3.	$0.2<t<1$	$P<1.0$	$E<0.27$	$\theta>75$	>299.7	<0.19	Interference between single and double scattering
4.	$1<t<10$	$P<4.2$	$E<2.7$	$\theta>50$	>297.3	<0.61	Double scattering
5.	$10<t<100$	$P<28.4$	$E<26.6$	$\theta>19.6$	>293.4	<2.0	
6.	$100<t$						

Table 3 Counting Rate

$$N = 3 \times 10^{17} \times 10^{4} \times 10^{13} \times \frac{d\sigma}{dt} \Delta t \frac{\Delta\phi}{2\pi} \text{ / jet pulse}$$

pp Elastic Scattering

$\|t\|$	$d\sigma/dt$	Δt	θ	$\sin\theta$	$\Delta\phi$	N / jet pulse	N /day**
1	1.5×10^{-30}	0.5	62°	0.88	0.028	102	3.3×10^{6}
2	4×10^{-32}	0.8	52.5°	0.79	0.032	4.8	1.6×10^{5}
4	3×10^{-33}	1.7	43.5°	0.69	0.036	0.88	3.0×10^{4}
10	$\sim1\times10^{-36}$	4	30.3°	0.50	0.050	0.001	33

pd Elastic Scattering

1	6×10^{-30}	0.8	75.5°	0.97	0.026	590	2.0×10^{8}
2	1×10^{-31}	1.0	69.3°	0.94	0.027	12	3.9×10^{5}
4	$\sim5\times10^{-35}$	1.7	61.5°	0.88	0.028	0.01	3.9×10^{2}

**

Note 1 These counting rates will be increased by a factor of 50 in the future,as mentioned in the text due to the improvement of the main ring beam and the jet target.

Note 2 For this calculation we assume 5 sec for a main ring cycle and three jets per pulse. Also we assume only two thirds of the total main ring pulses are available due to the sublimation of jet and other miscellaneous things.

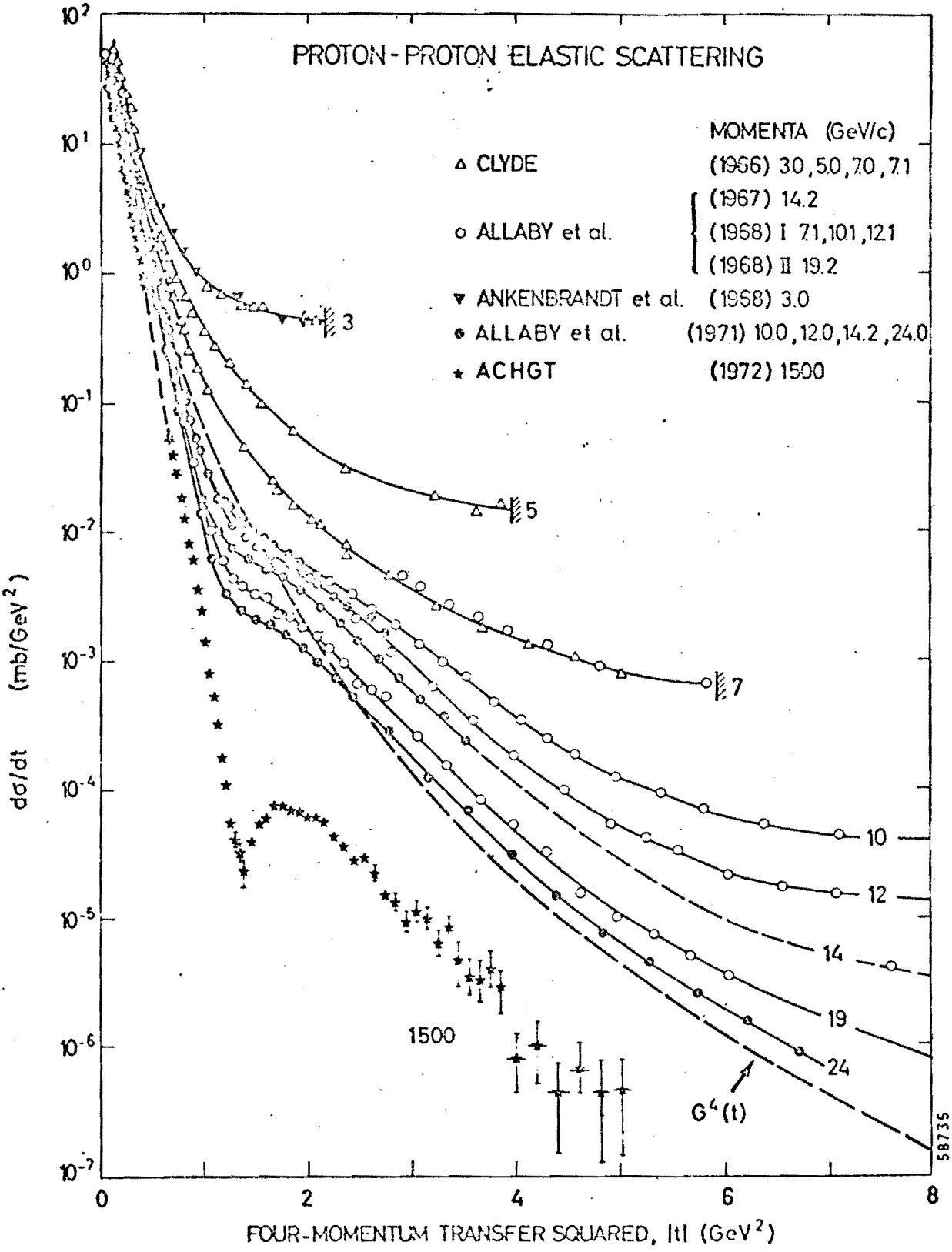

Fig. 1 Proton-Proton Elastic Scattering

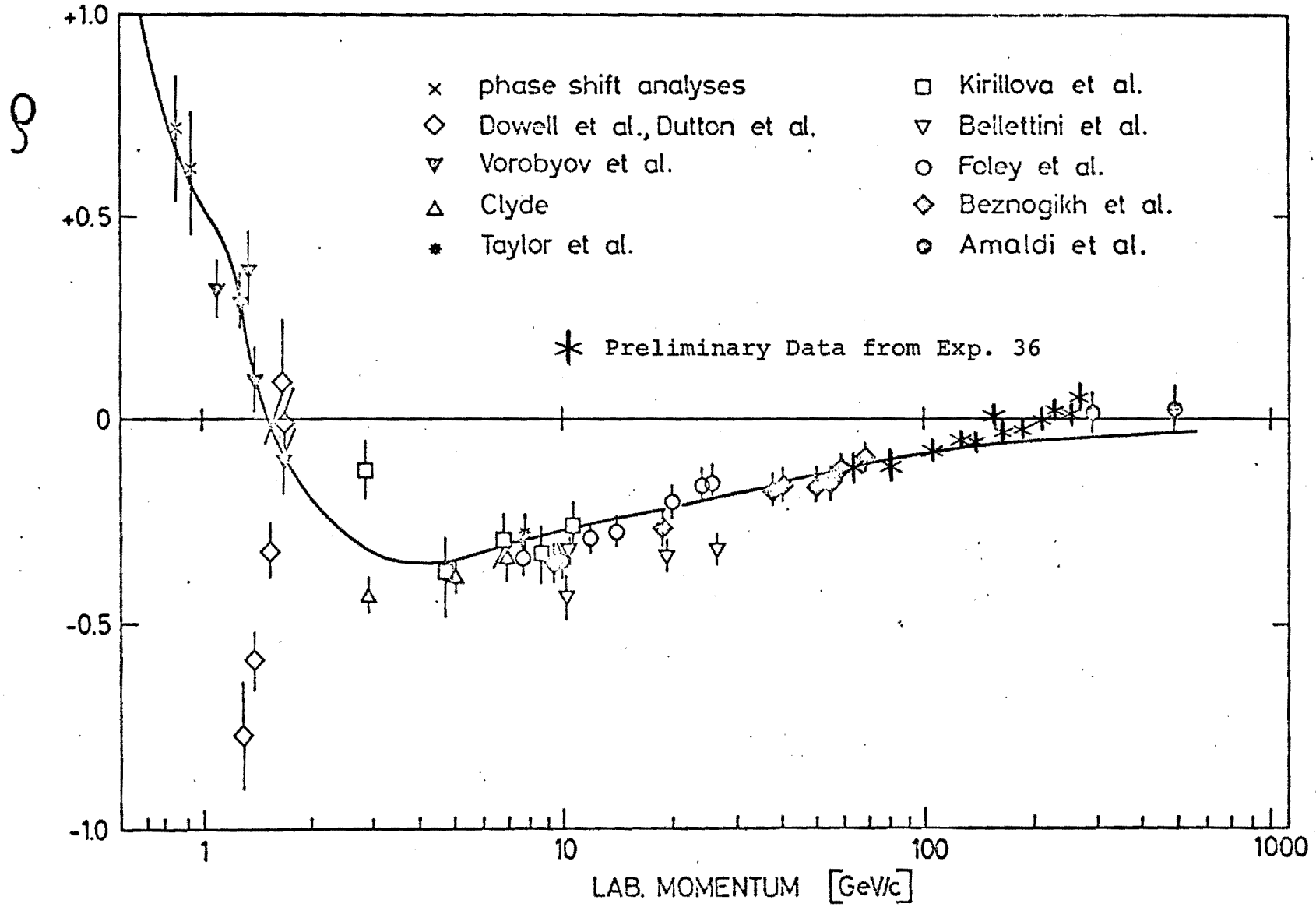

Fig. 2 Ratio of Real Part to Imaginary Part of Scattering Amplitude

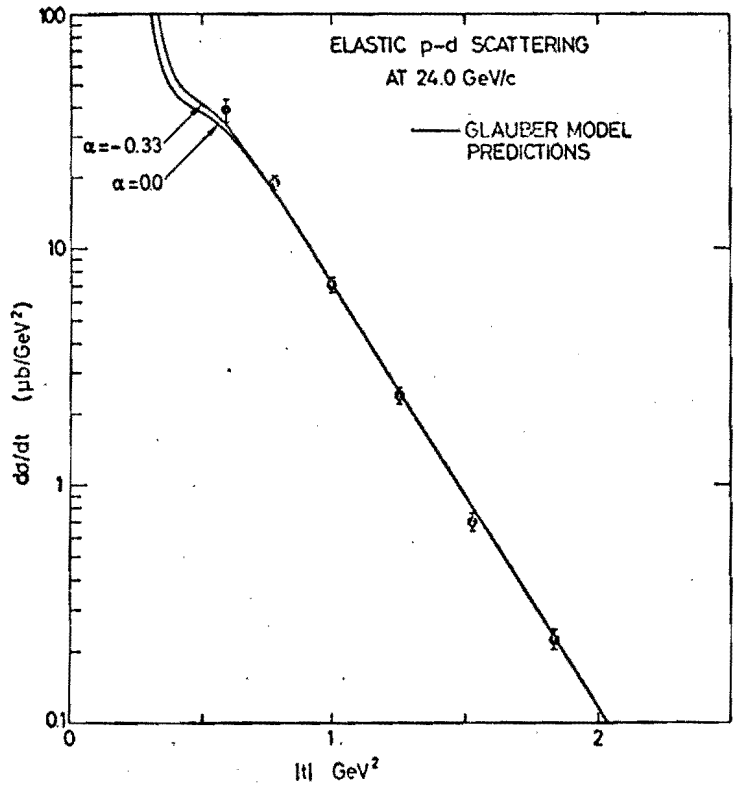

The results of elastic p – d scattering at 24.0 GeV/*c* are shown versus four-momentum transfer squared, |*t*|. The curves are Glauber-model calculations of elastic p – d scattering for two values of the ratio α of the real to the imaginary part of the p – p and p – n scattering amplitude.

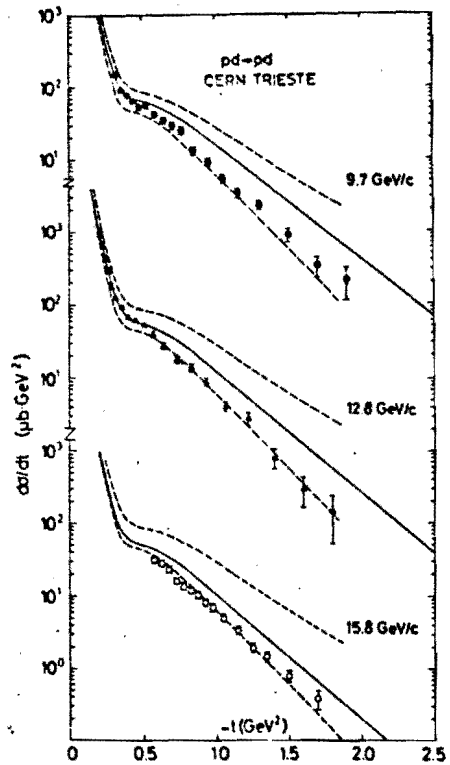

The pd elastic differential cross-section at 9.7 (‡), 12.8 (†), and 15.8 (§) GeV/*c*.

Fig. 3 p-d Elastic Scattering

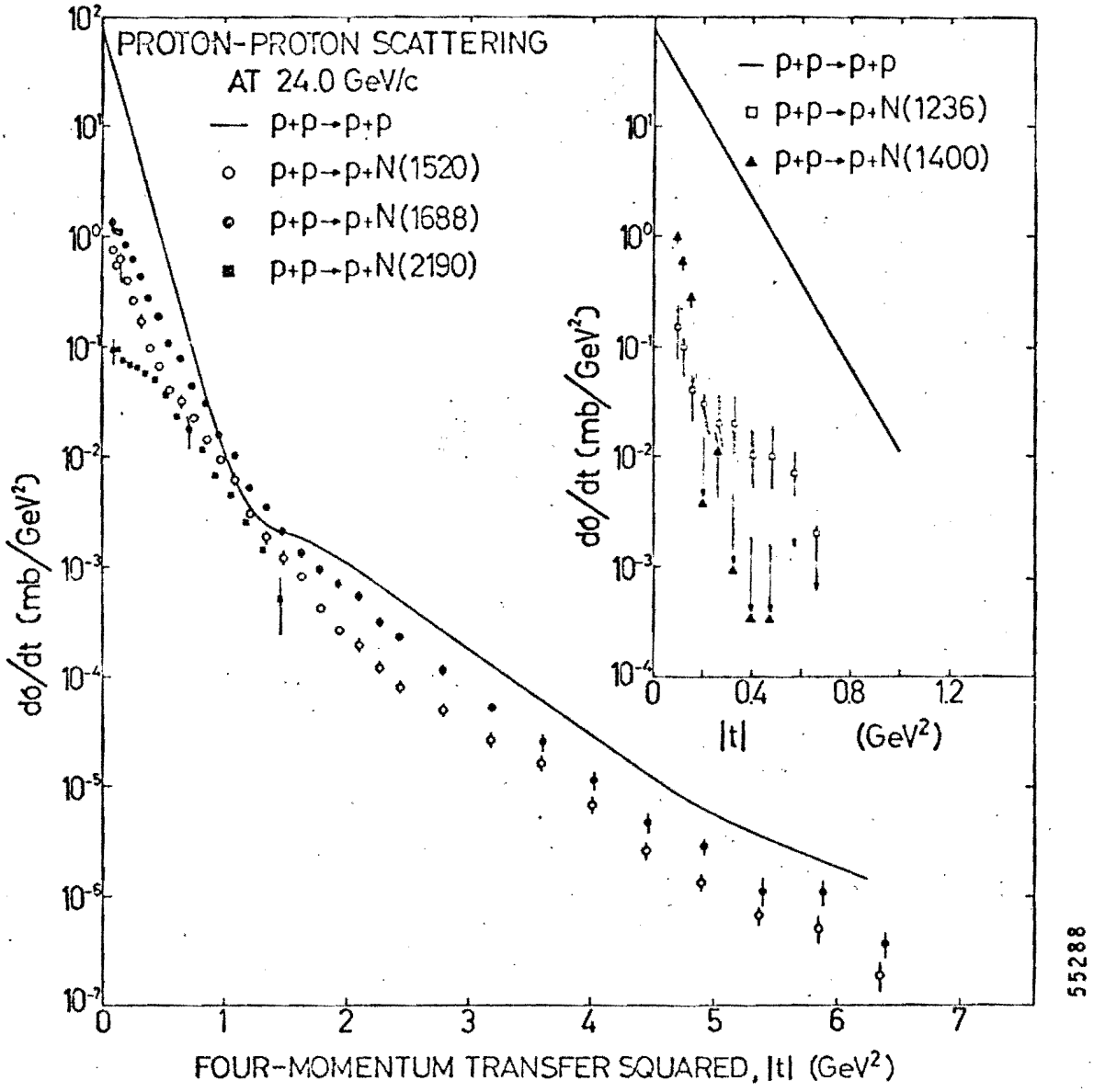

Fig. 4 Isobar Production at 24 GeV/c

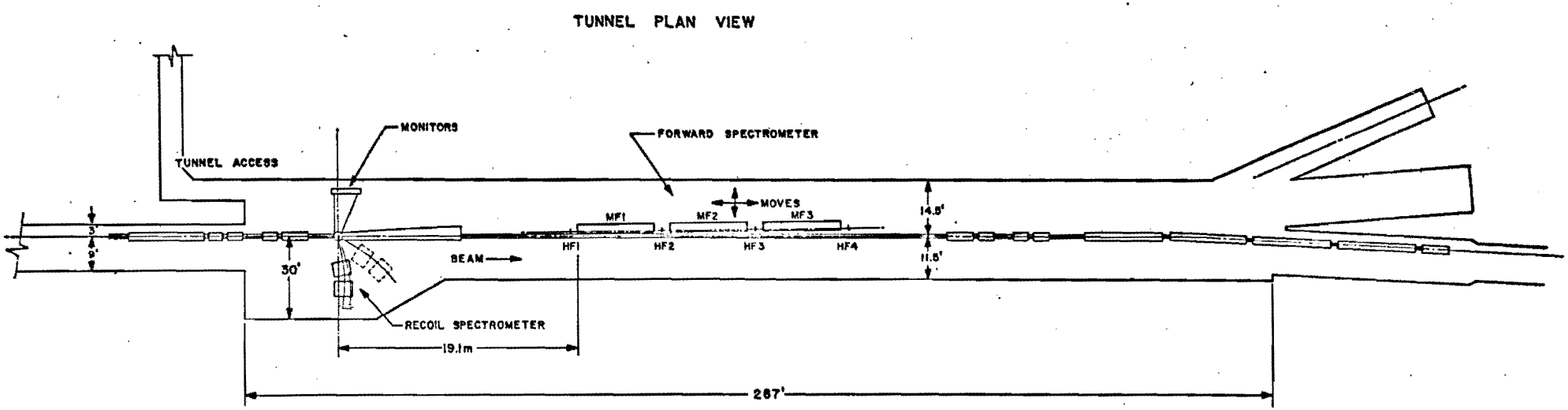

FIG. 5 GENERAL LAYOUT OF PROPOSED EXPERIMENT IN BO STRAIGHT SECTION

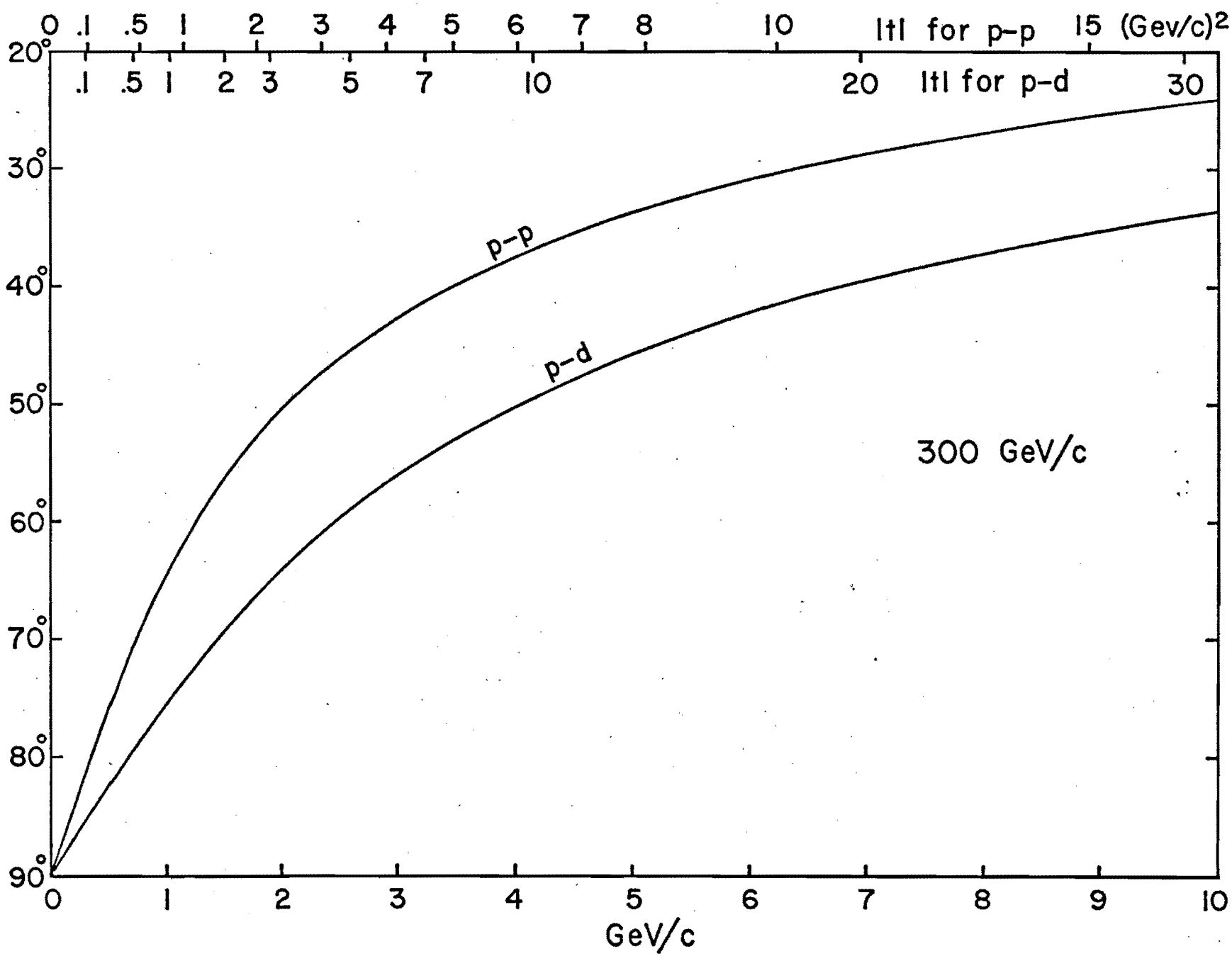

FIG. 6 KINEMATICS OF RECOIL PARTICLES

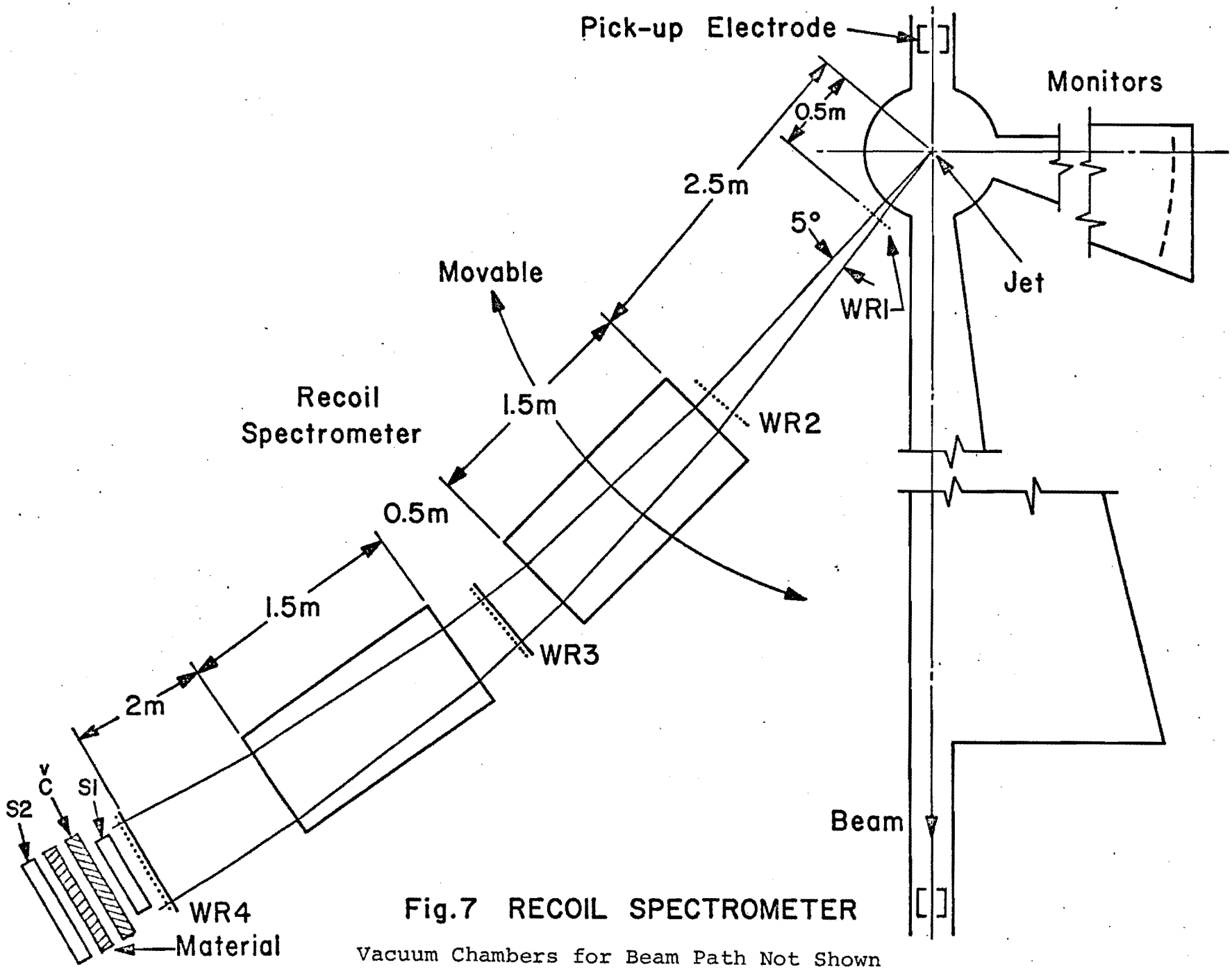

Fig.7 RECOIL SPECTROMETER

Vacuum Chambers for Beam Path Not Shown

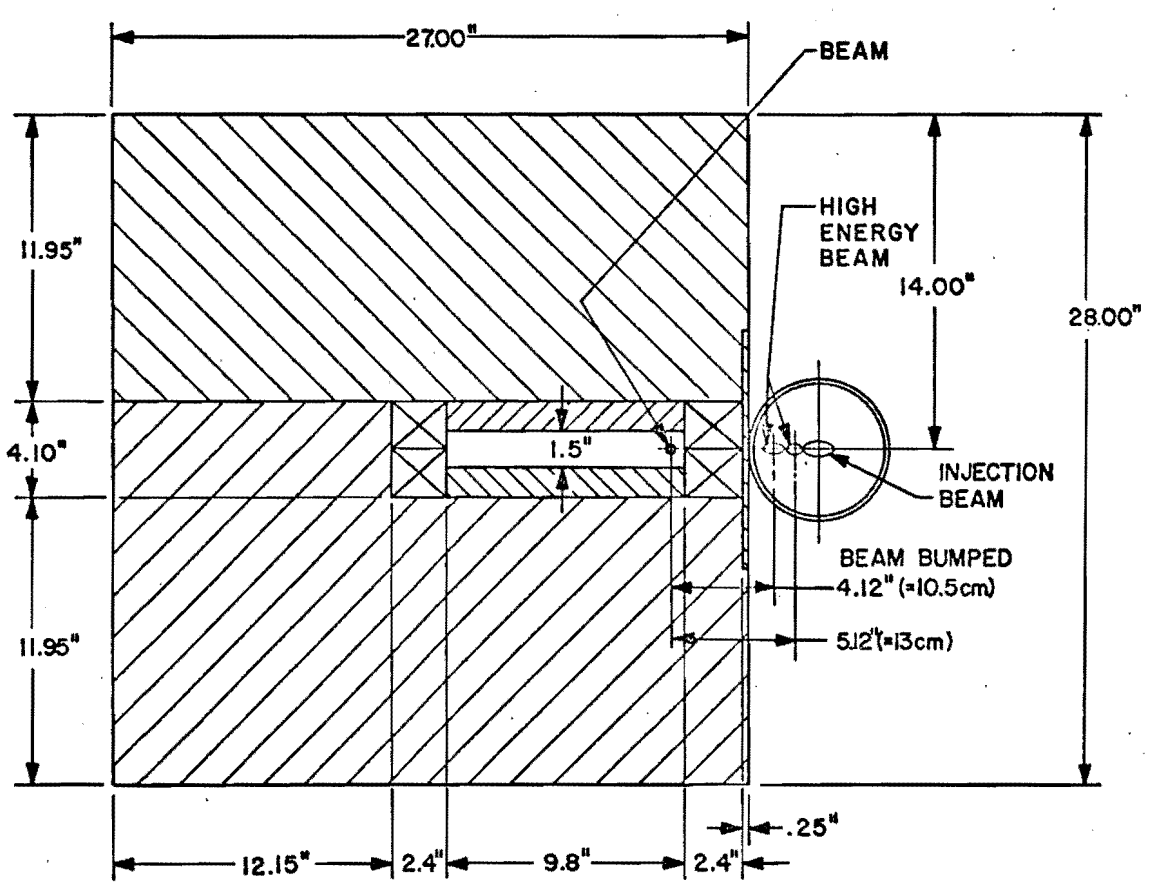

FIG. 8B CROSS SECTION of FORWARD MAGNET

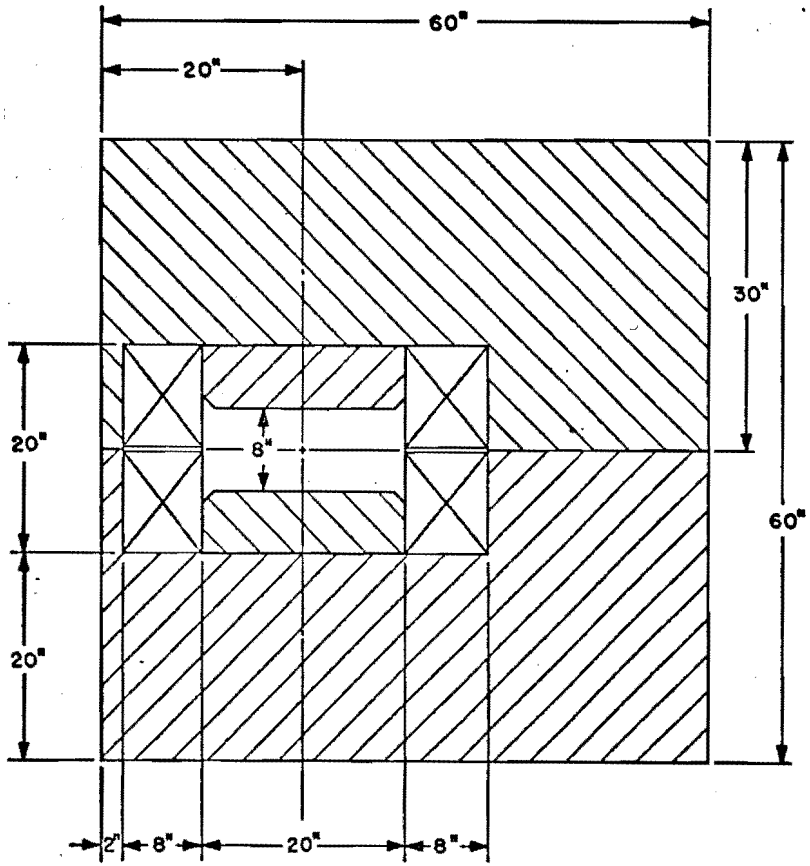

FIG. 8A CROSS SECTION of RECOIL MAGNET

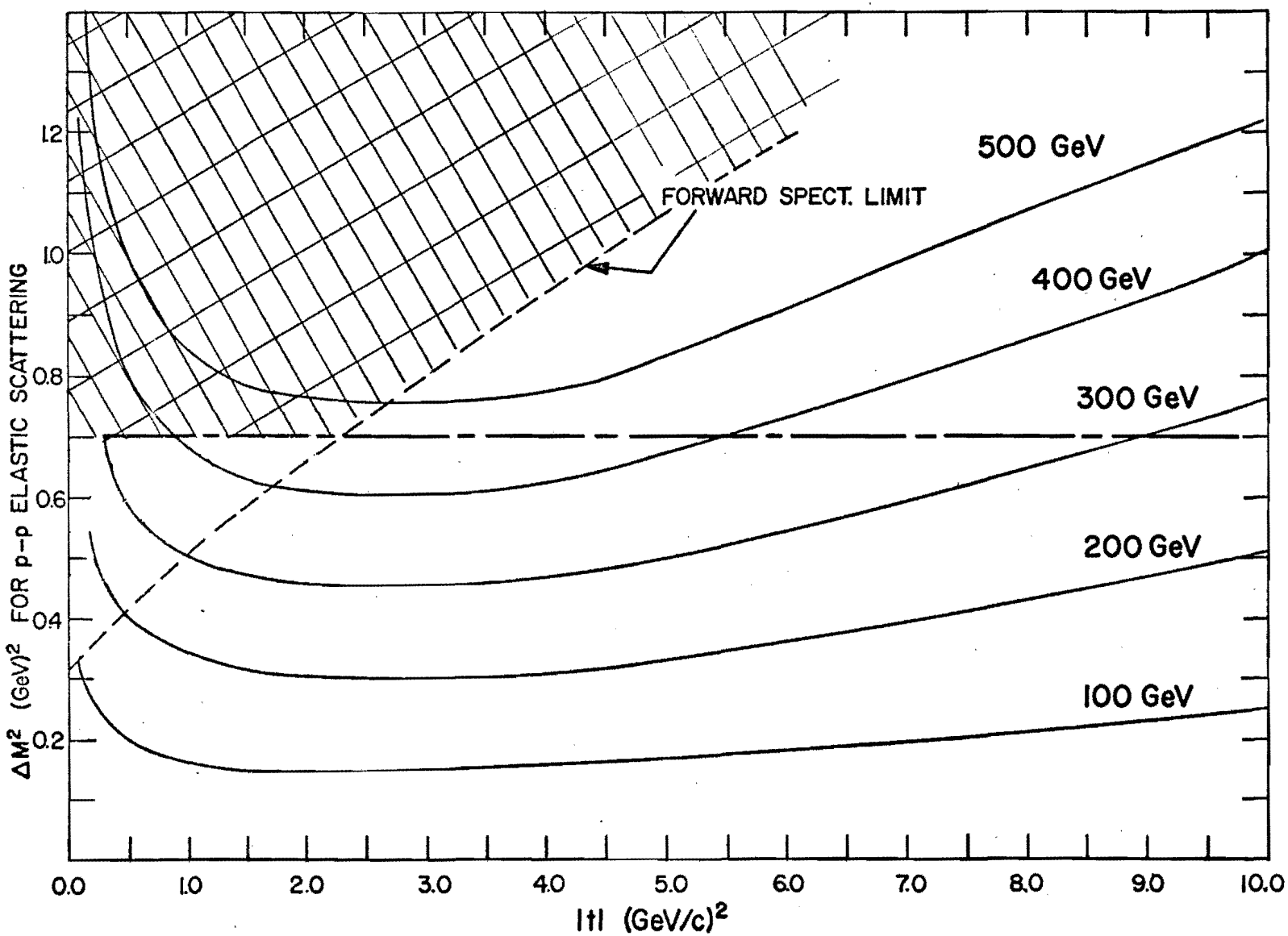

Figure 9A. Missing Mass Squared Resolution as a Function of $|t|$ for p-p Elastic Scattering.

The dashed line represents the geometric boundary of the forward spectrometer. Points below $\Delta M^2 = 0.7\,(\mathrm{GeV})^2$ (broken line) are accessible with the recoil spectrometer only. Hence, only the crosshatched region is inaccessible to this experiment.

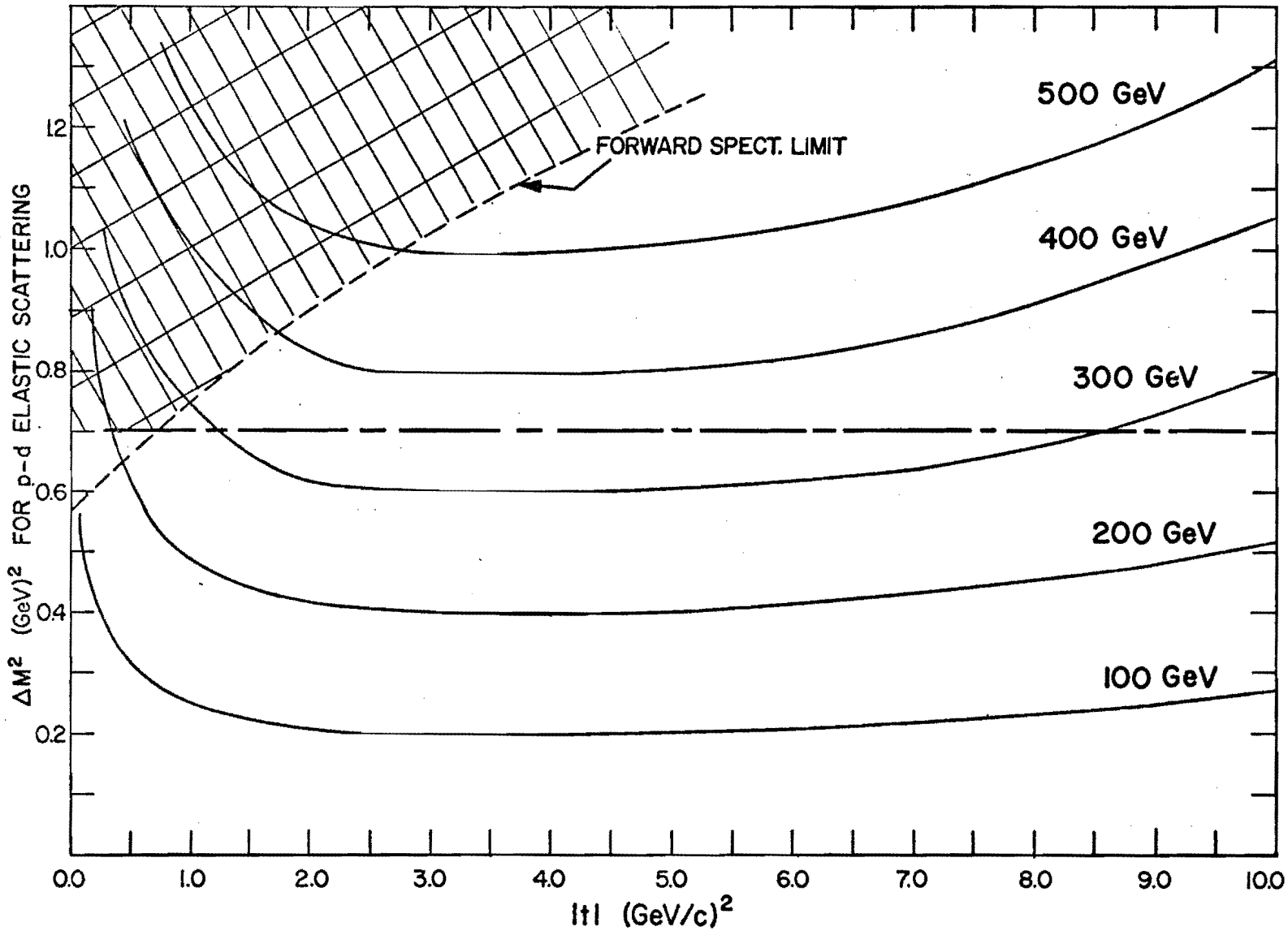

Figure 9B. Missing Mass Squared Resolution as a Function $|t|$ for p-d Elastic Scattering.

The dashed line represents the geometric boundary of the forward spectrometer. Points below $\Delta M^2 = 0.7$ $(GeV)^2$ (broken line) are accessible with the recoil spectrometer only. Hence, only the crosshatched region is inaccessible to this experiment.

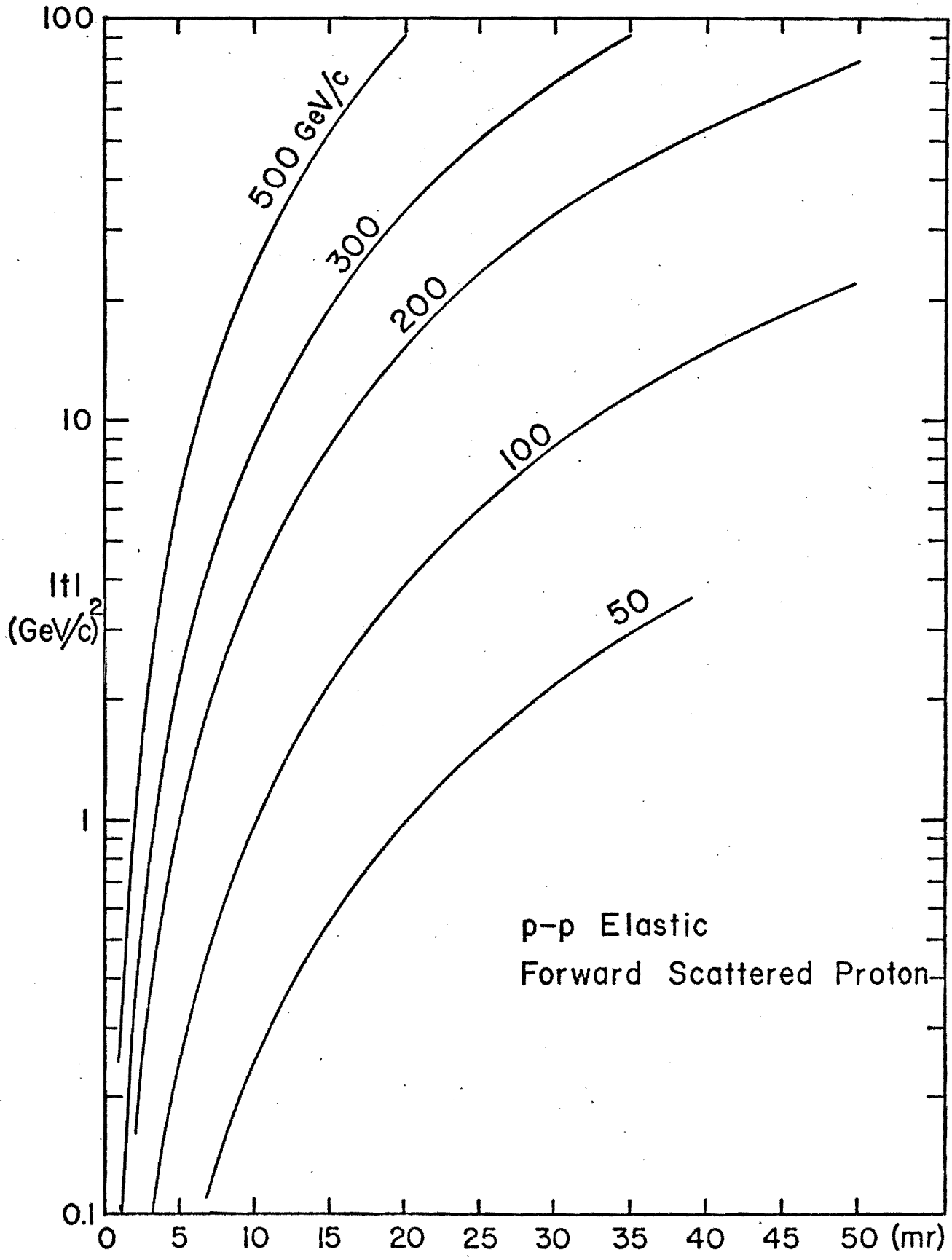

FIG. 10 KINEMATICS OF FORWARD SCATTERED PROTON

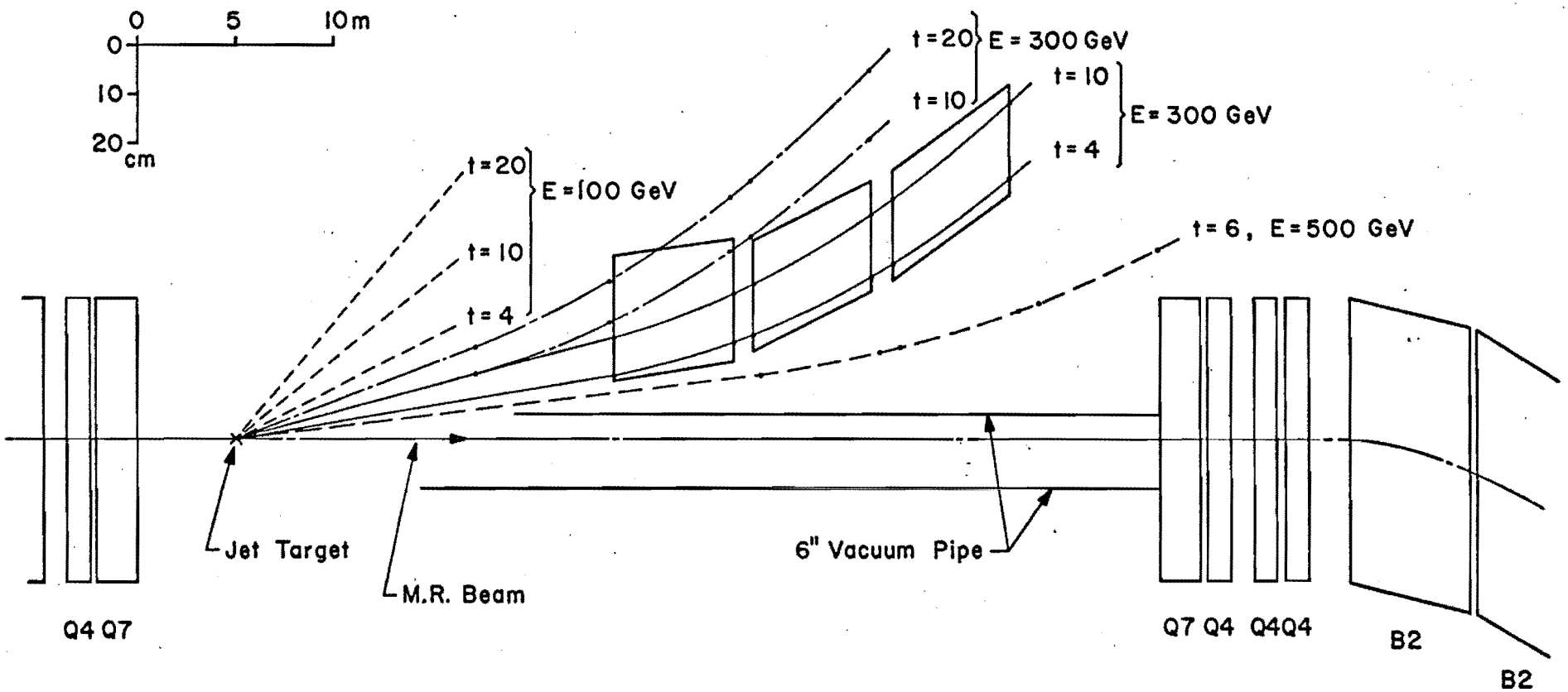

Fig. 11 Position of Forward Spectrometer

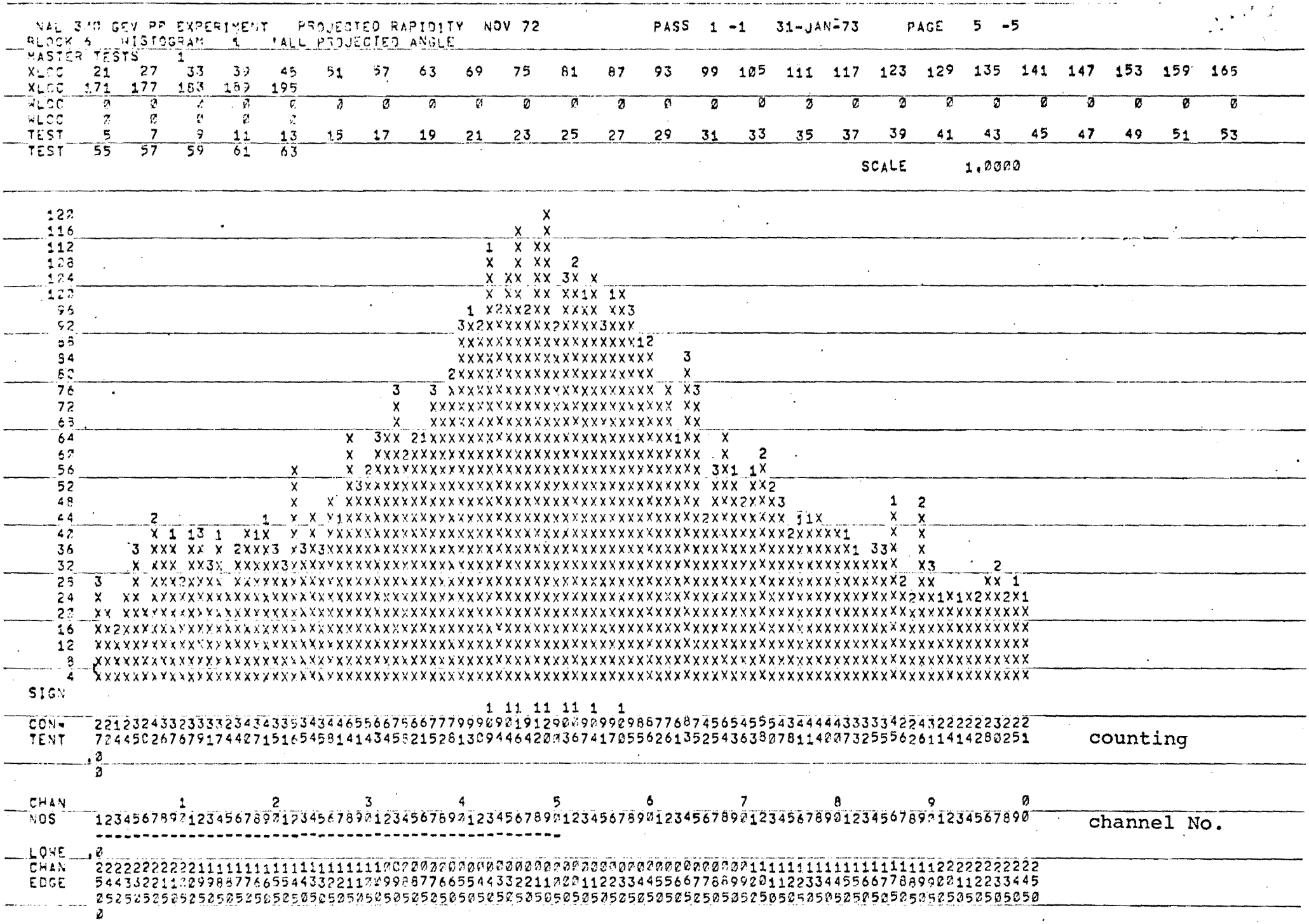

Fig. 12 Projected Angular Distribution of p-p reaction at 303 GeV/d in units of 5 mr